Electronic Supplementary Material (ESI) for Polymer Chemistry.

Supporting Information to:

"Controlling the Synthesis of Degradable Vinyl Polymers by Xanthate-Mediated Polymerization"

Craig A. Bell,[a,b,c] Guillaume G. Hedir,[a] Rachel K. O'Reilly[a]* and Andrew P. Dove[a]*

[a] Department of Chemistry, University of Warwick, Gibbet Hill, Coventry, CV4 7AL, UK

[b] Australian Institute for Bioengineering and Nanotechnology, The University of Queensland, St Lucia, Queensland, 4072, Australia.

[c] Centre for Advanced Imaging, The University of Queensland, St Lucia, Queensland, 4072, Australia.

Corresponding Authors

* r.k.o-reilly@warwick.ac.uk; a.p.dove@warwick.ac.uk

Table of Contents

Small molecule analogues

Below are the small molecule analogues that shows the ^{13}C NMR chemical shift of the proposed functionality before and after Z-group fragmentation.[1, 2]

S-butyl-*O*-butyl xanthate

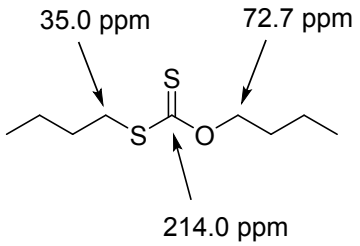

S,S-dibutyl carbonodithioate

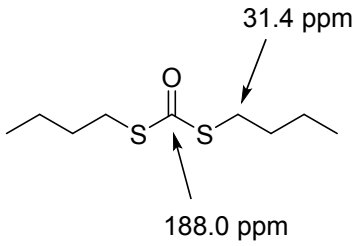

Small Molecule characterization

O-*p*-methoxyphenyl-*S*-methylacetylxanthate (CTA 2)

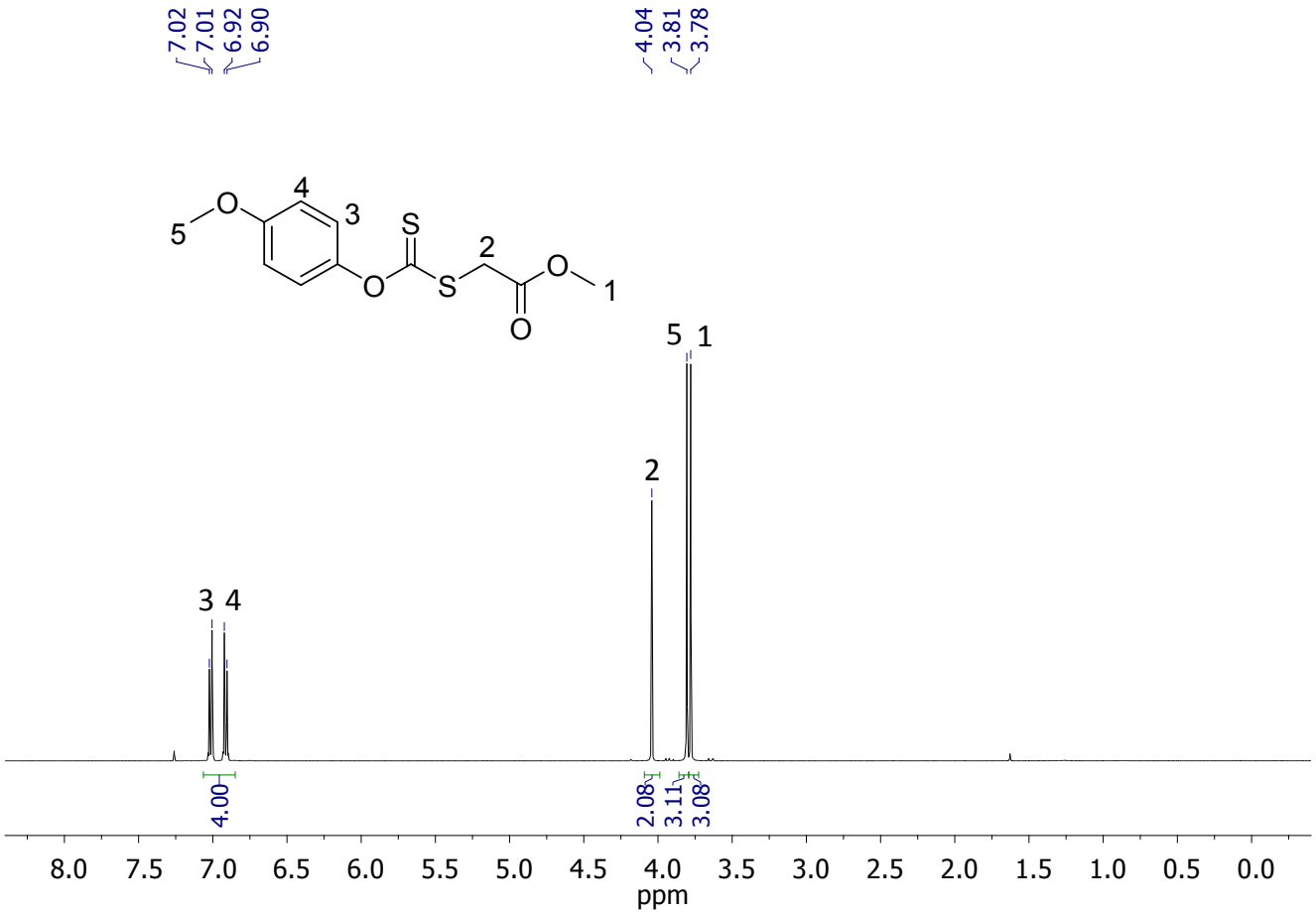

Figure S1 - ^{1}H NMR spectrum of CTA **2** (500 MHz, $CDCl_3$).

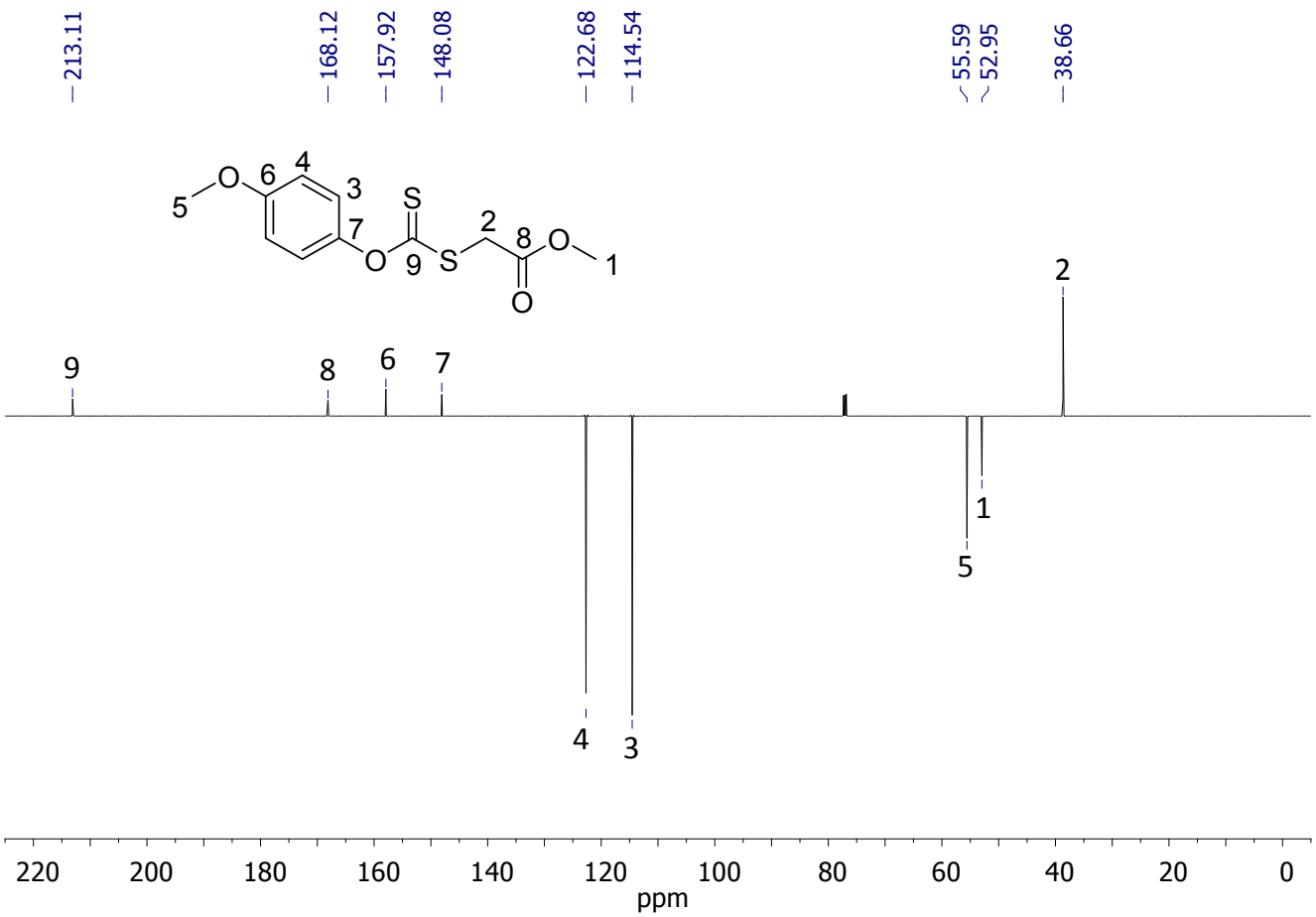

Figure S2 - ^{13}C APT NMR spectrum of CTA **2** (125 MHz, $CDCl_3$).

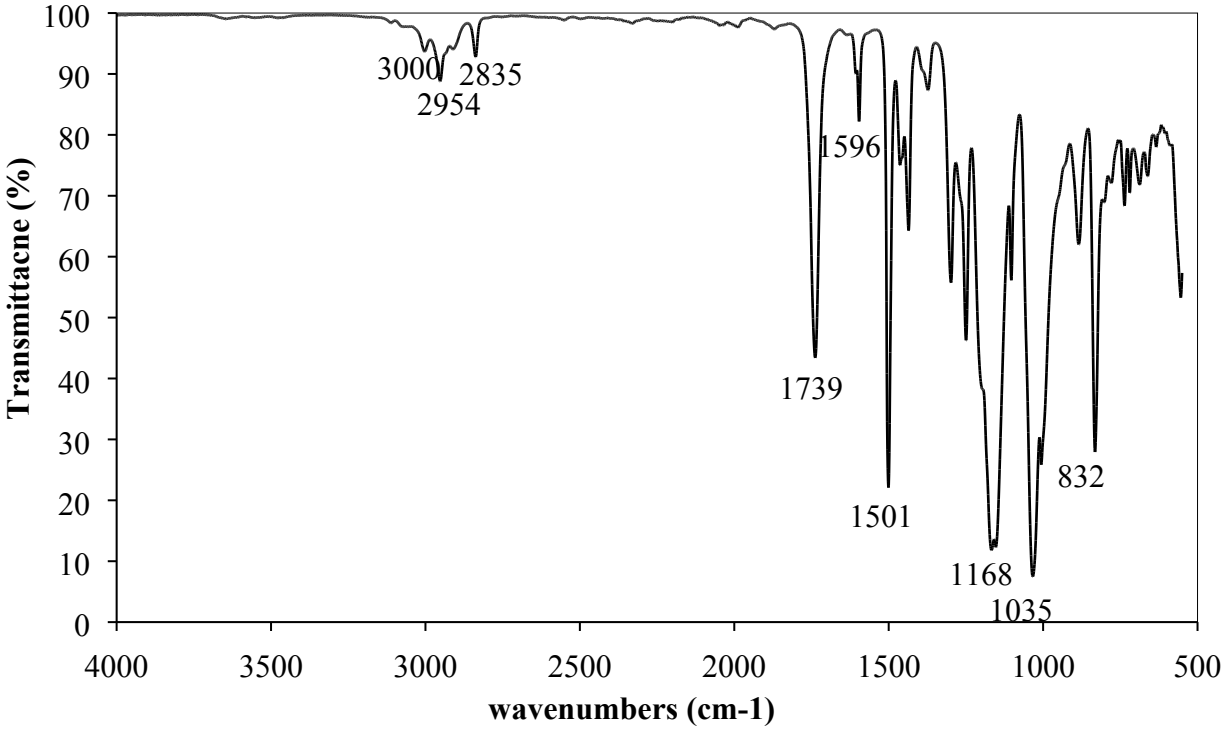

Figure S3 - ATR-FTIR spectrum of CTA **2.**

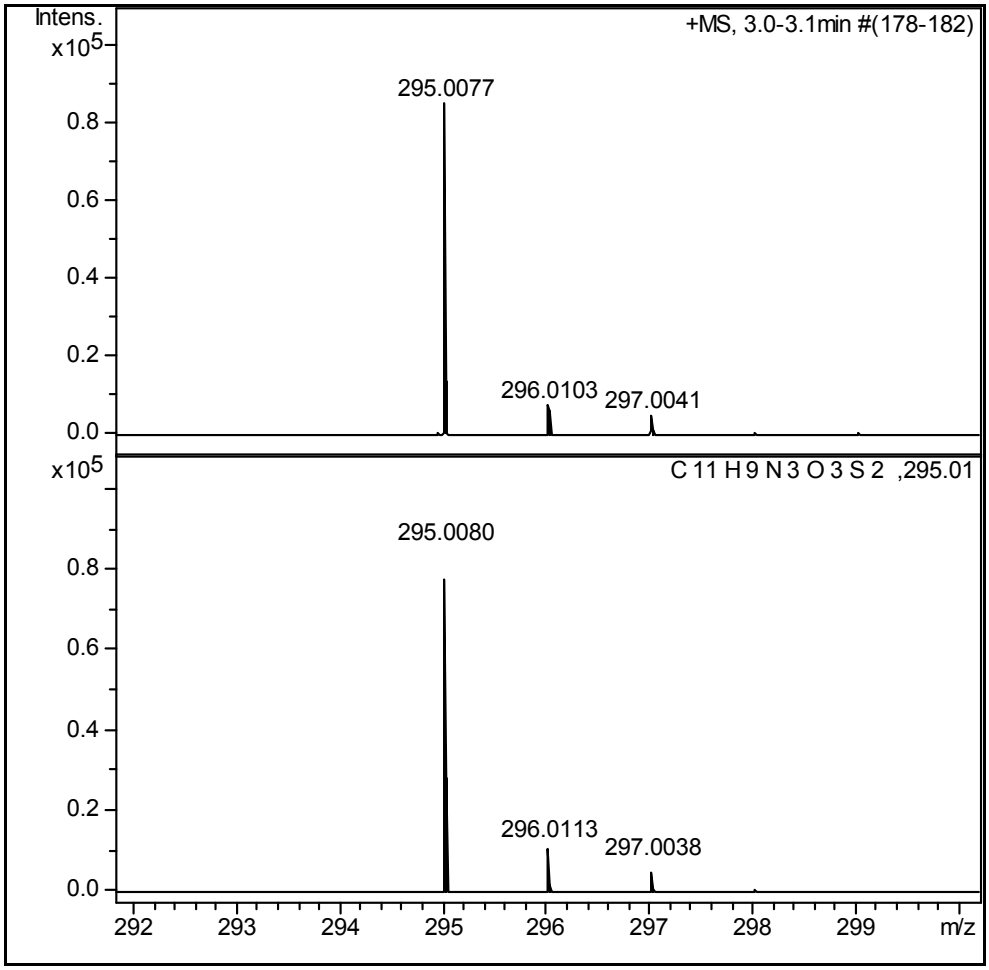

Figure S4 - HRMS analysis of CTA **2** (top: observed/bottom: simulated).

***O*-n-hexyl-*S*-methyl 2-propionylxanthate (CTA 1)**

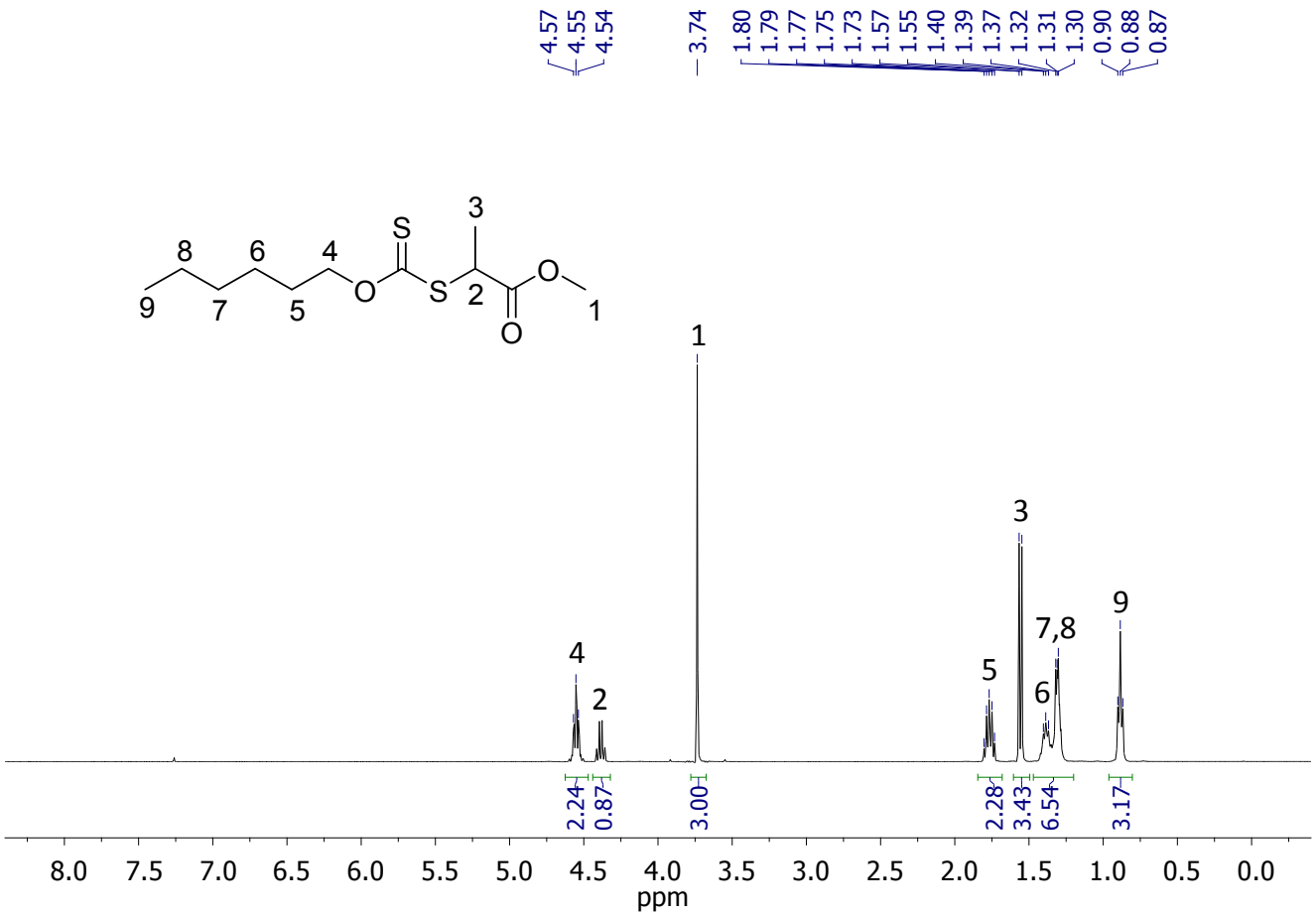

Figure S5 - ^{1}H NMR spectrum of CTA **1** (400 MHz, $CDCl_3$).

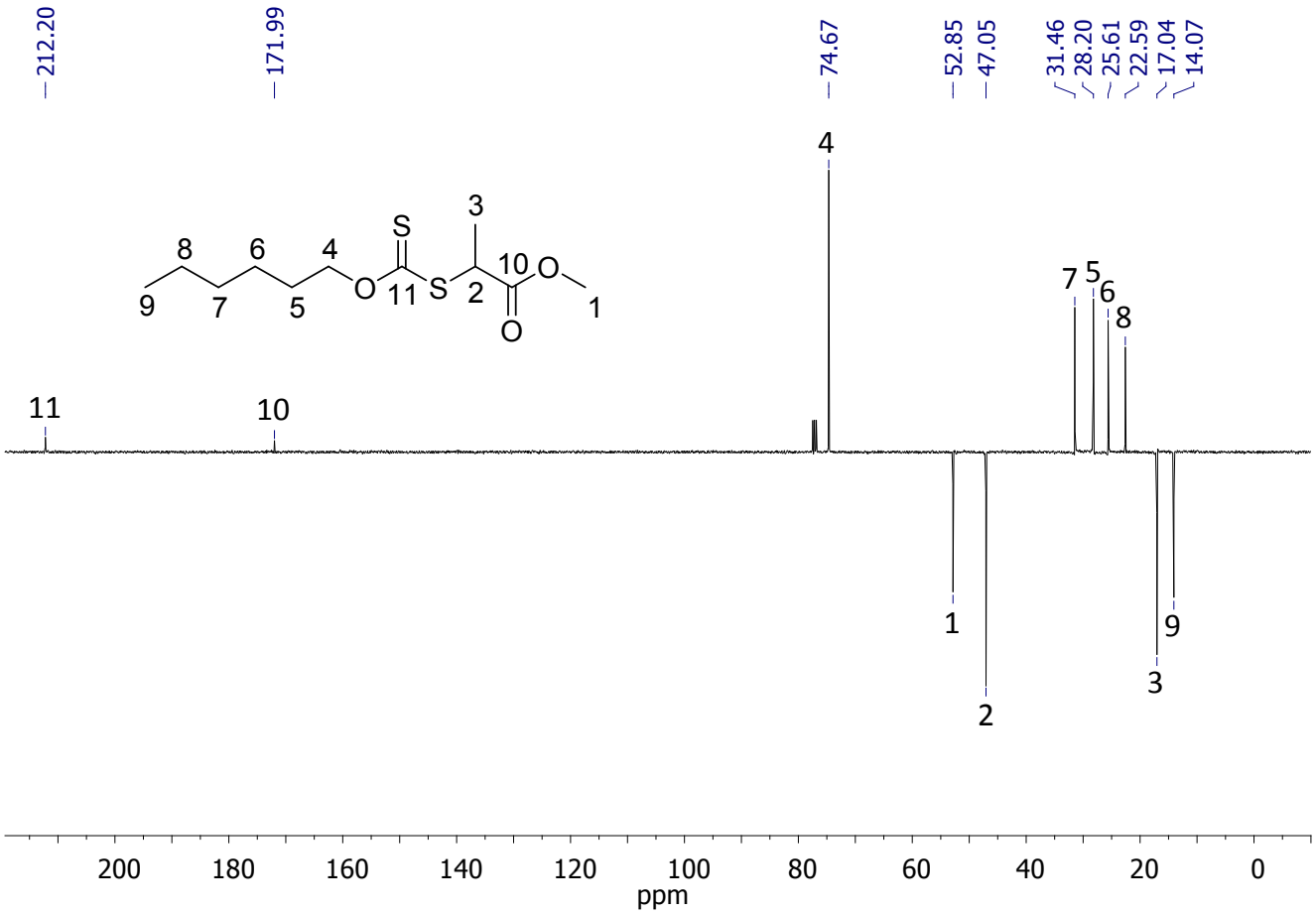

Figure S6 - ^{13}C APT NMR spectrum of CTA **1** (100 MHz, $CDCl_3$).

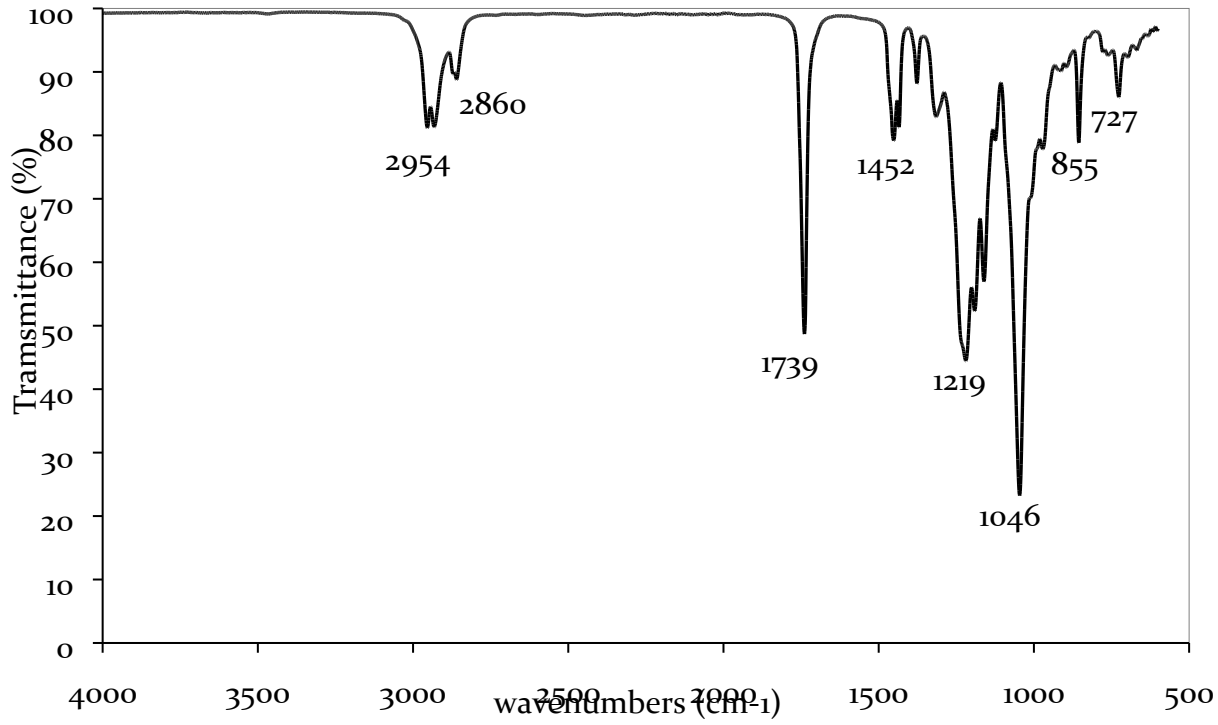

Figure S7 - ATR-FTIR spectrum of CTA **1.**

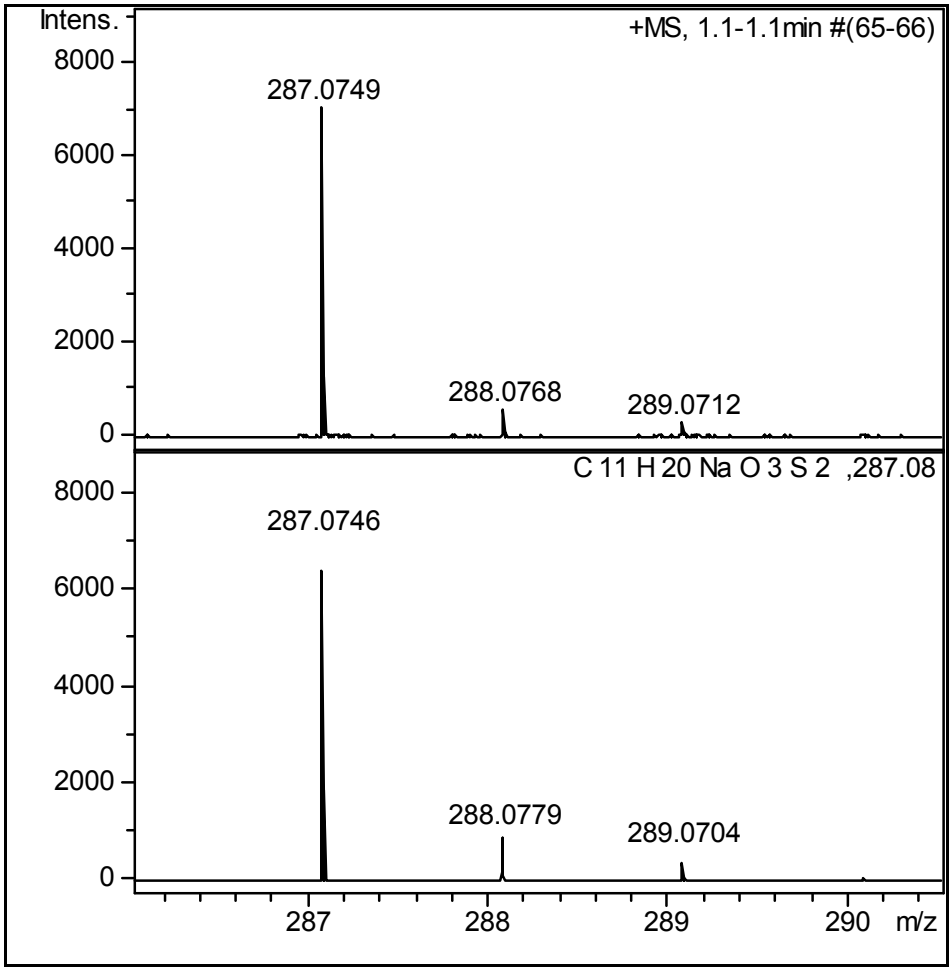

Figure S8 - HRMS analysis of CTA **1** (top: observed/bottom: simulated).

***O*-isopropyl-*S*-methyl 2-propionylxanthate (CTA 4)**

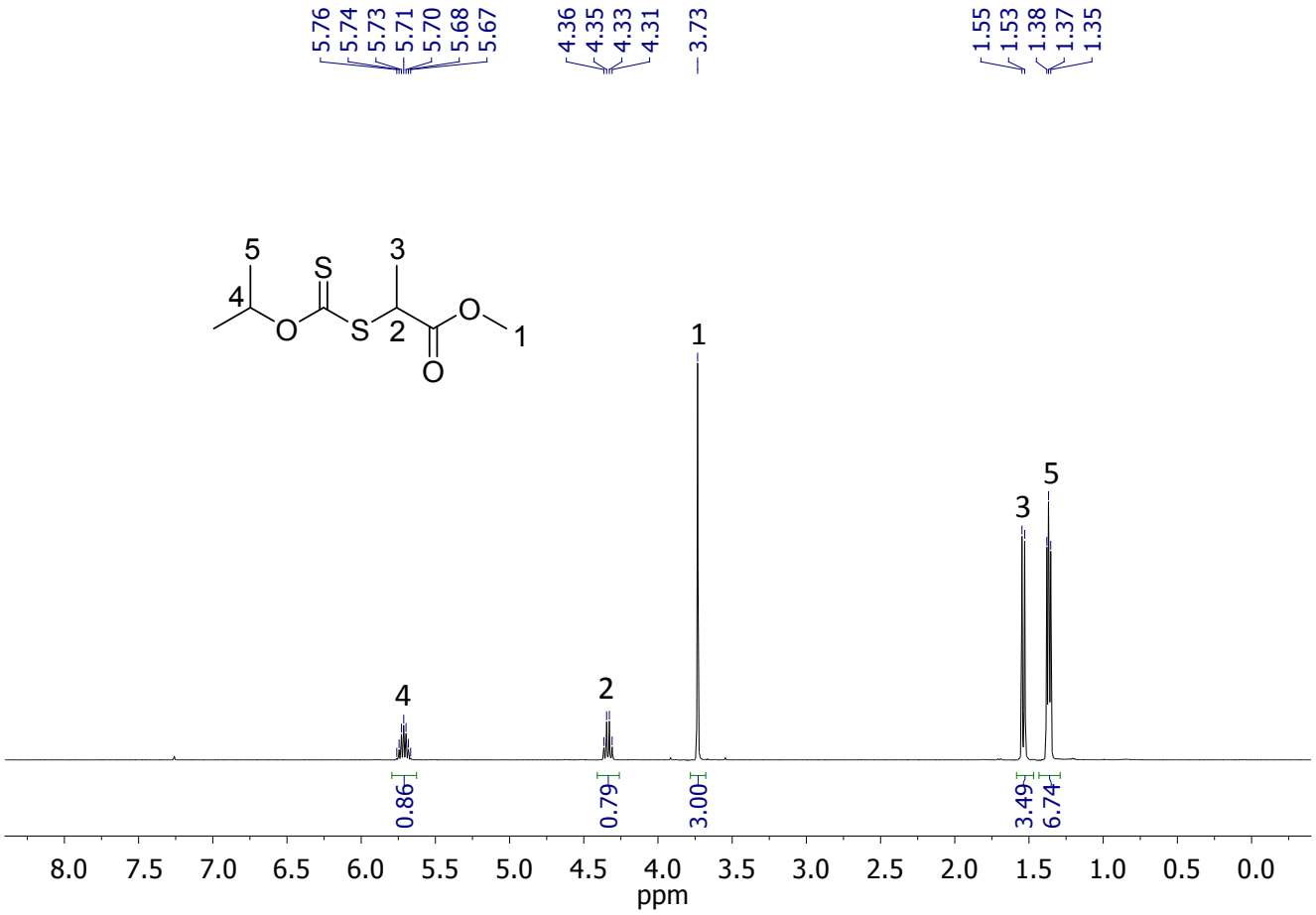

Figure S9 - ^{1}H NMR spectrum of CTA **4** (400 MHz, $CDCl_3$).

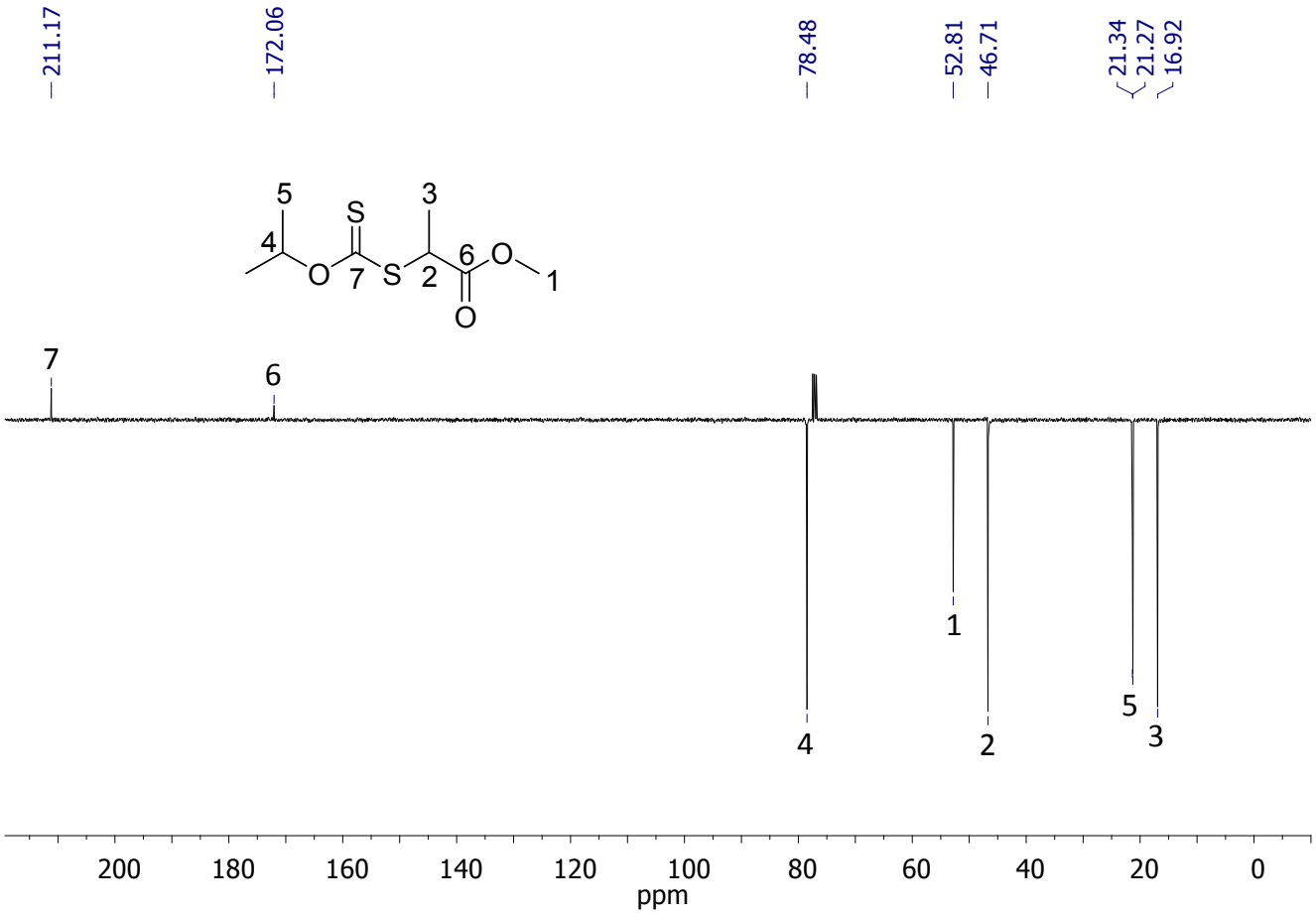

Figure S10 - ^{13}C APT NMR spectrum of CTA **4** (100 MHz, $CDCl_3$).

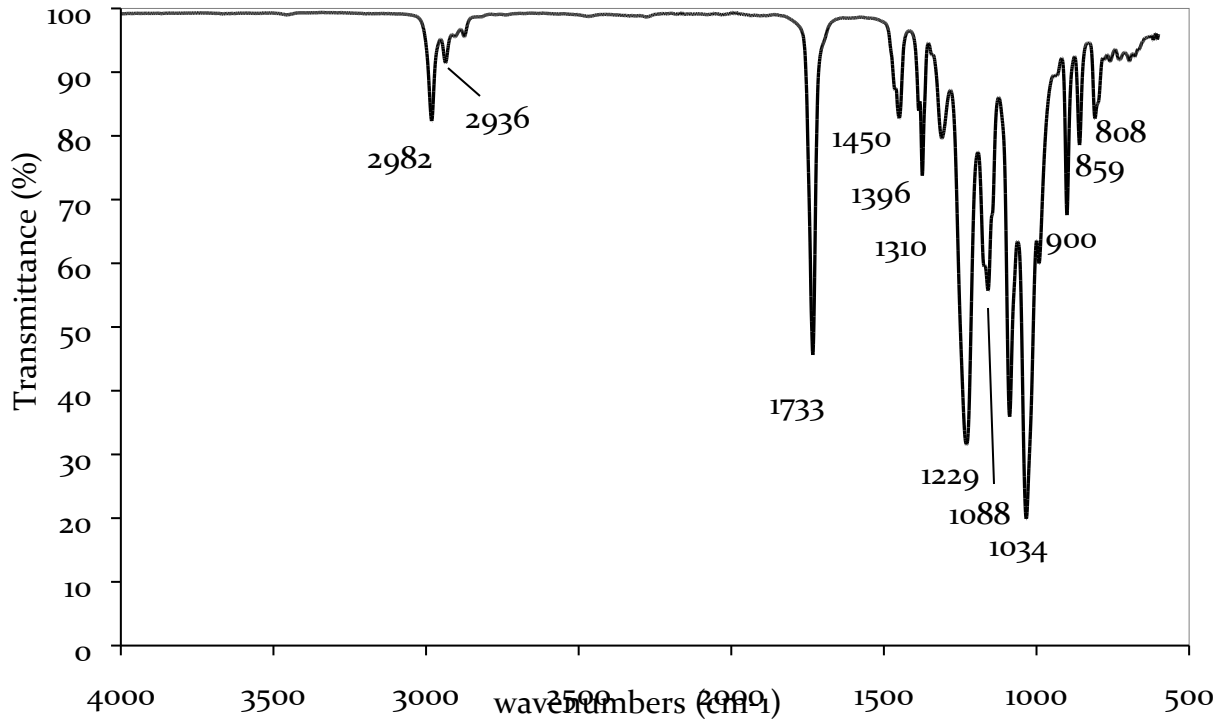

Figure S11 - ATR-FTIR spectrum of CTA **4.**

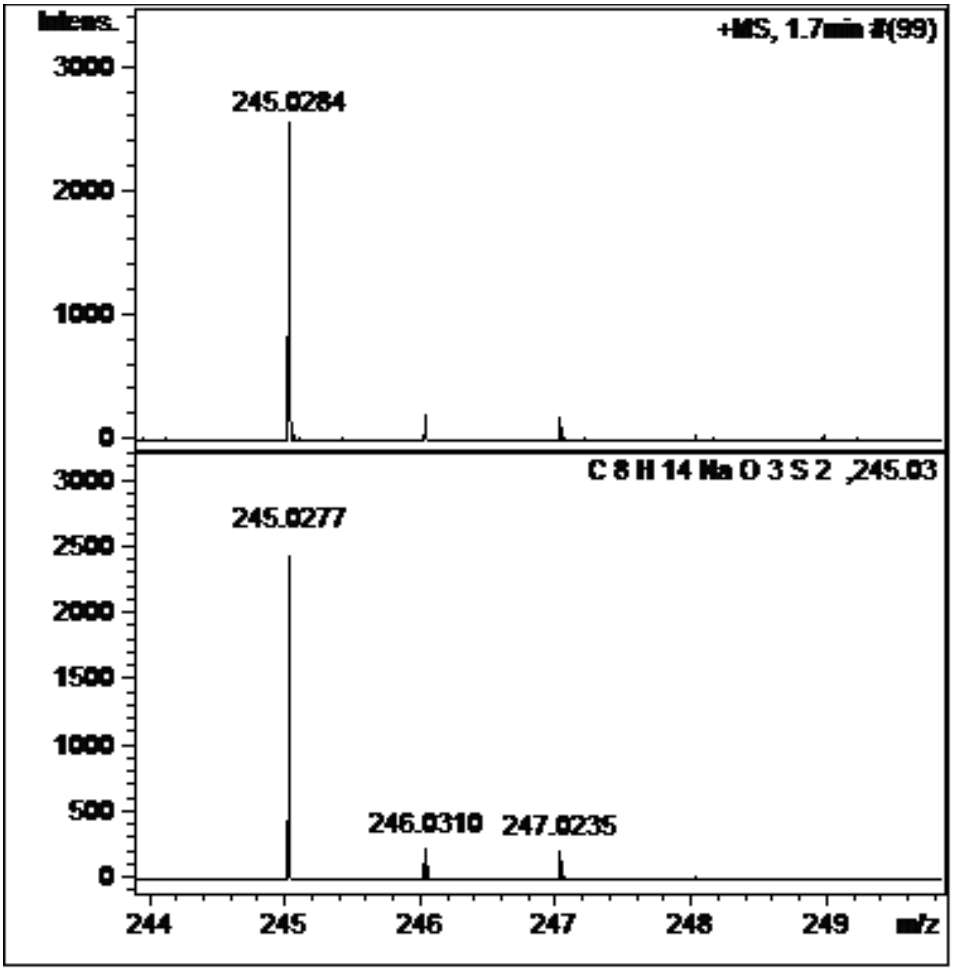

Figure S12 - HRMS analysis of CTA **4** (top: observed/bottom: simulated).

Polymer Synthesis

Polymer Characterization - SEC, ^{1}H NMR, ^{13}C NMR analysis

Poly(VAc$_{0.93}$-co-MDO$_{0.07}$)$_{79}$ formed using CTA 2

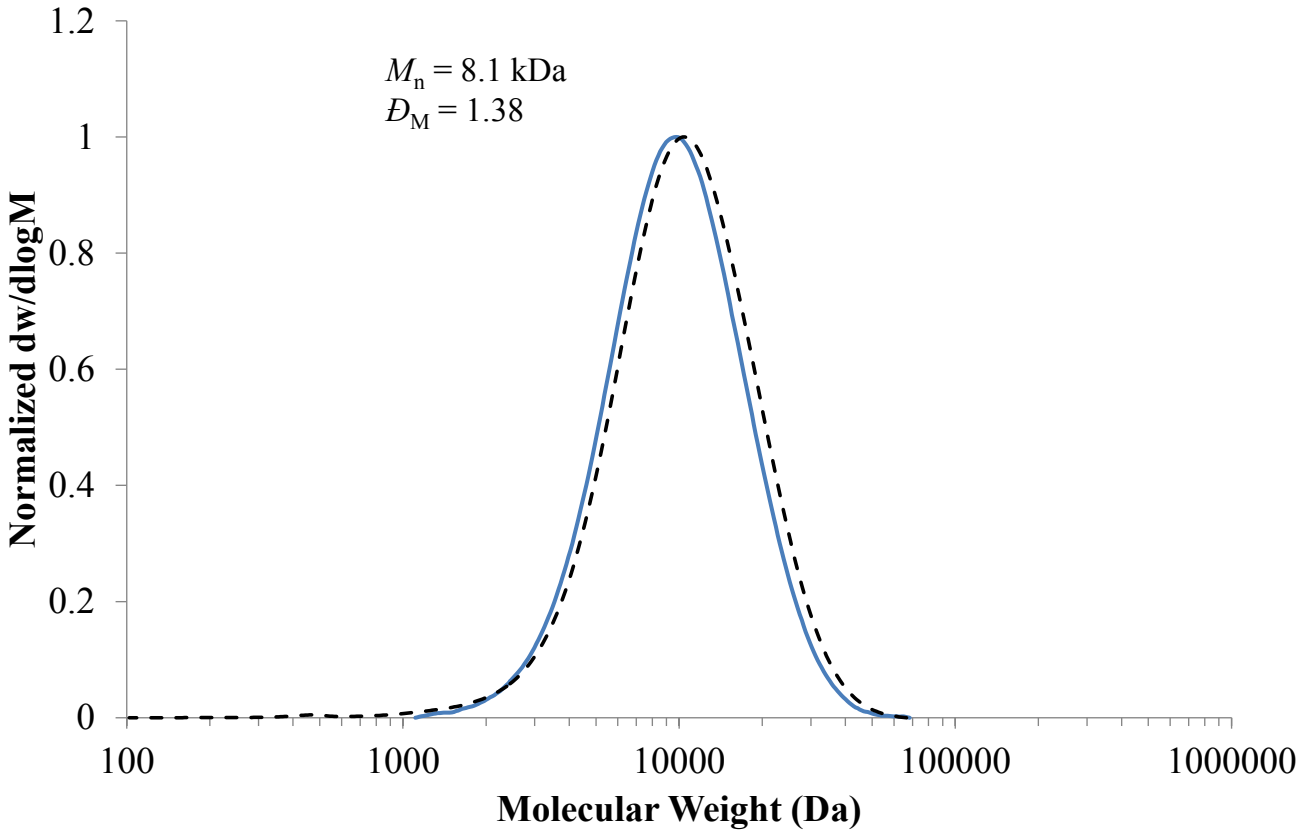

Figure S13 – SEC chromatogram of P(VAc$_{0.93}$-co-MDO$_{0.07}$)$_{79}$ formed using **CTA 2** (90 °C, 4 h). Monomer conversion: VAc = 58 %, MDO = 51 %, M_n = 8.1 kDa, $Đ_M$ = 1.38 (SEC $CHCl_3$, based on PS standards). Dashed line indicates the weight distribution obtained from the UV detector @ 280 nm.

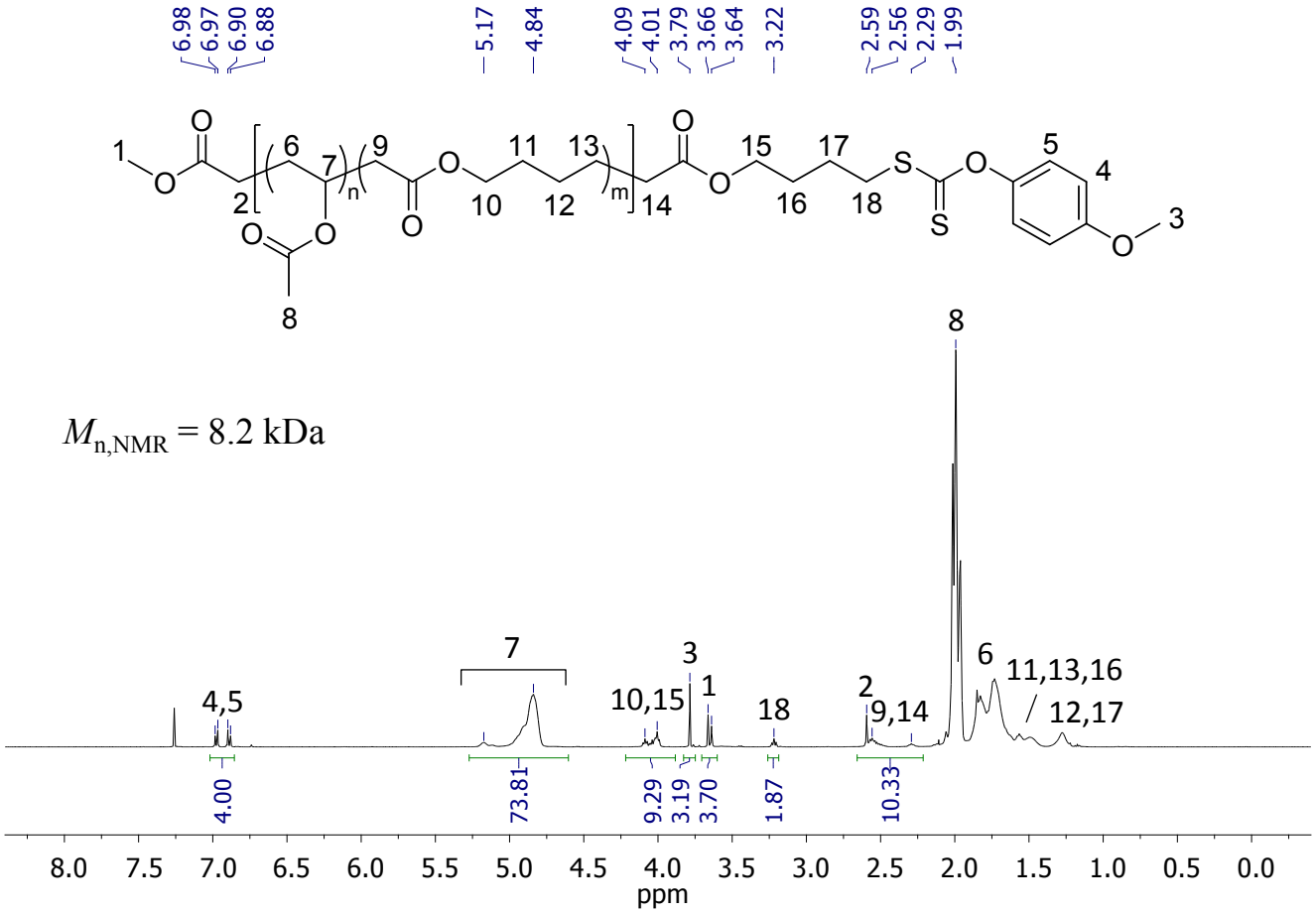

Figure S14 – ^{1}H NMR spectrum of P(VAc$_{0.93}$-co-MDO$_{0.07}$)$_{79}$ formed using **CTA 2** (500 MHz, $CDCl_3$).

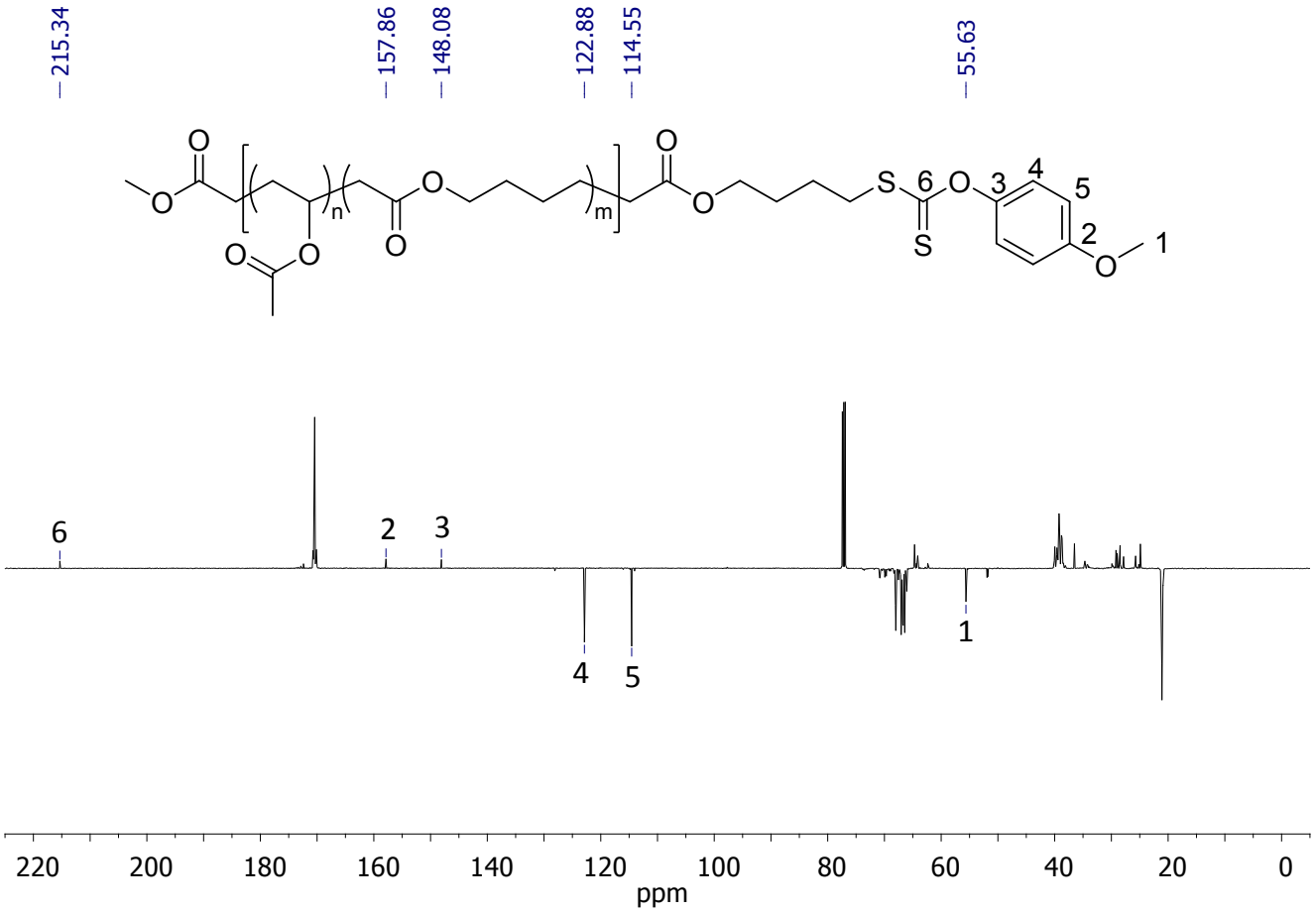

Figure S15 – ^{13}C APT NMR spectrum of $P(VAc_{0.93}\text{-co-}MDO_{0.07})_{79}$ formed using **CTA 2** (125 MHz, $CDCl_3$).

Poly($VAc_{0.79}$-co-$MDO_{0.21}$)$_{75}$ formed using CTA 2

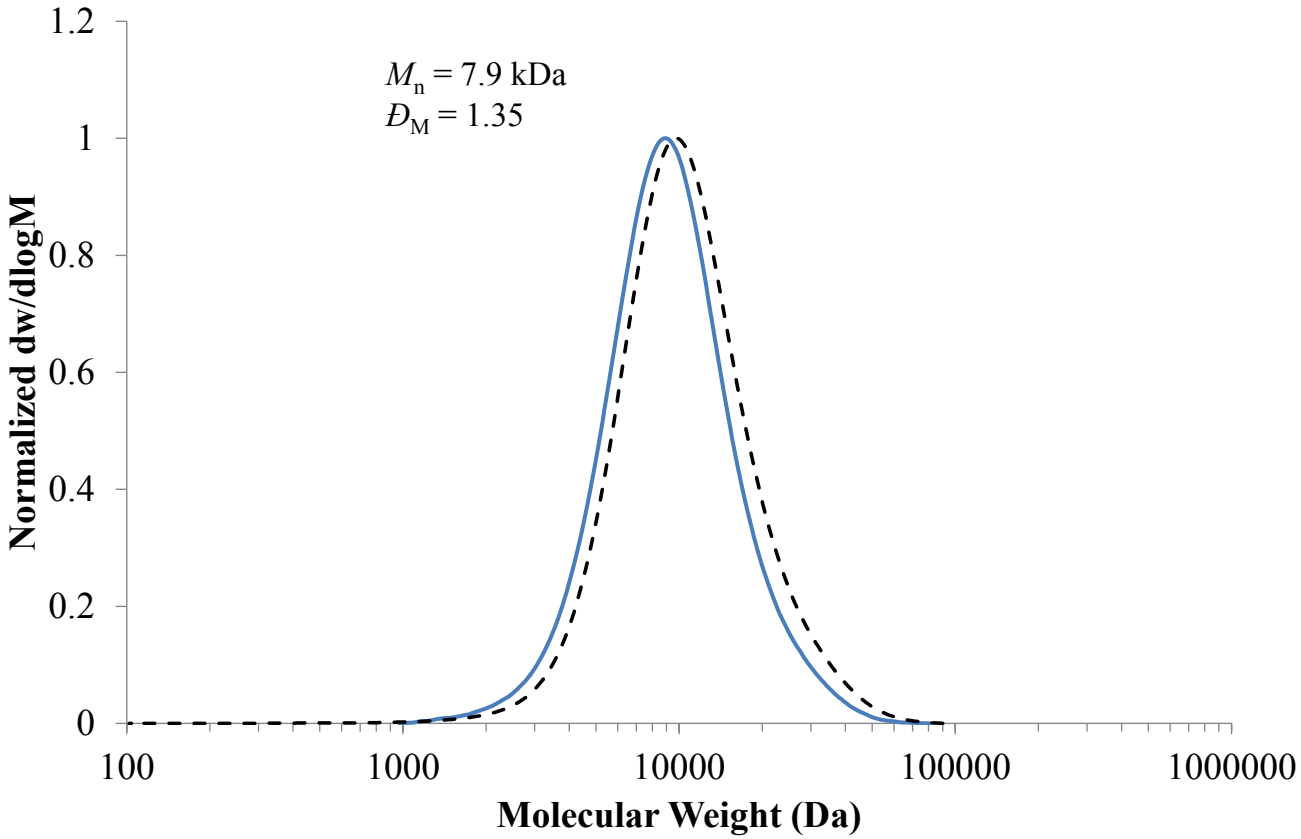

Figure S16 – SEC chromatogram of P($VAc_{0.79}$-co-$MDO_{0.21}$)$_{75}$ formed using **CTA 2** (90 °C, 15 h). Monomer conversion: VAc = 65 %, MDO = 41 %, M_n = 7.9 kDa, $Đ_M$ = 1.35 (SEC $CHCl_3$, based on PS standards). Dashed line indicates the weight distribution obtained from the UV detector @ 280 nm.

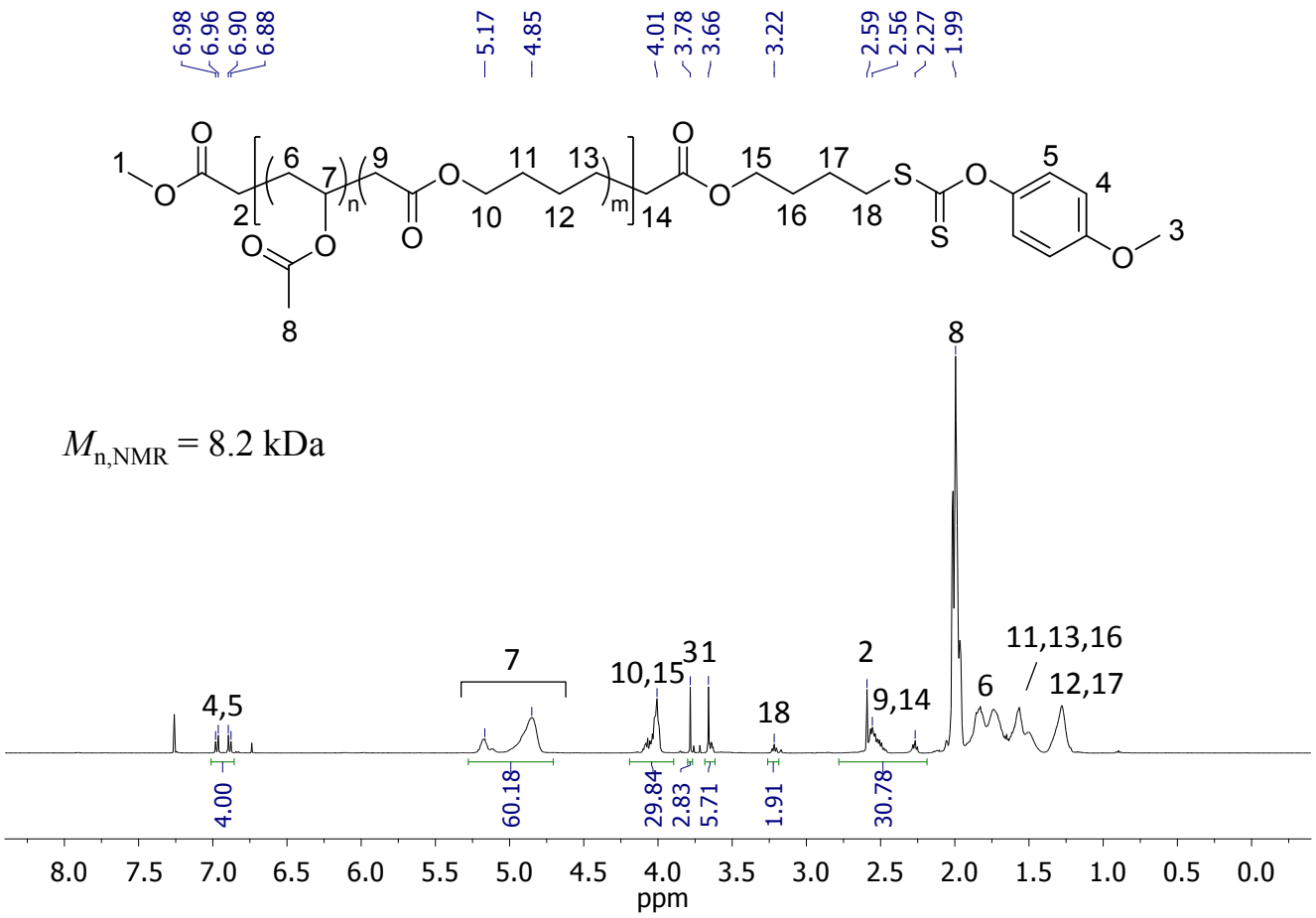

Figure S17 – ^{1}H NMR spectrum of P(VAc$_{0.79}$-co-MDO$_{0.21}$)$_{75}$ formed using **CTA 2** (500 MHz, $CDCl_3$).

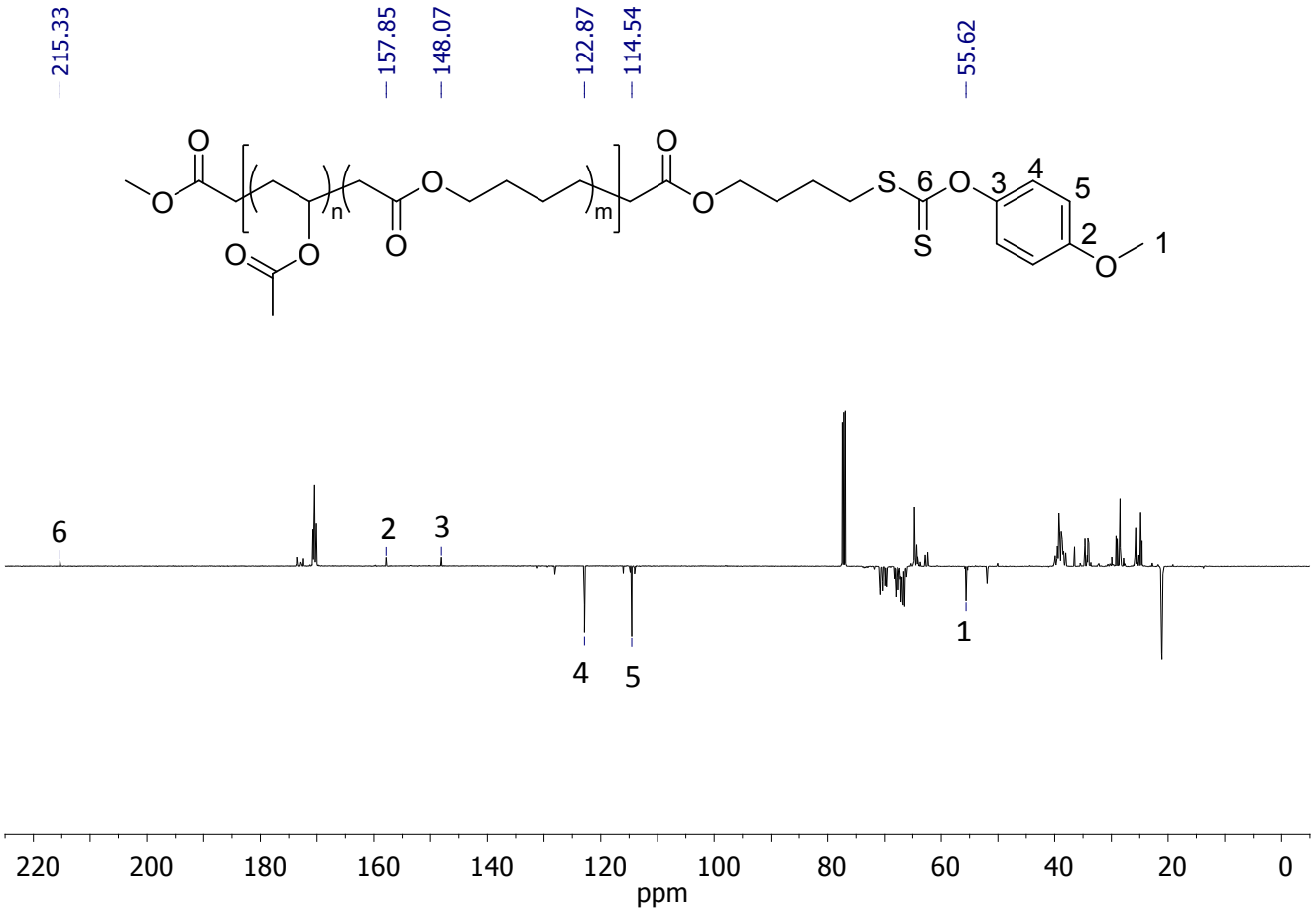

Figure S18 – ^{13}C APT NMR spectrum of $P(VAc_{0.79}\text{-co-}MDO_{0.21})_{75}$ formed using **CTA 2** (125 MHz, $CDCl_3$).

Poly($VAc_{0.66}$-co-$MDO_{0.34}$)$_{60}$ formed using CTA 2

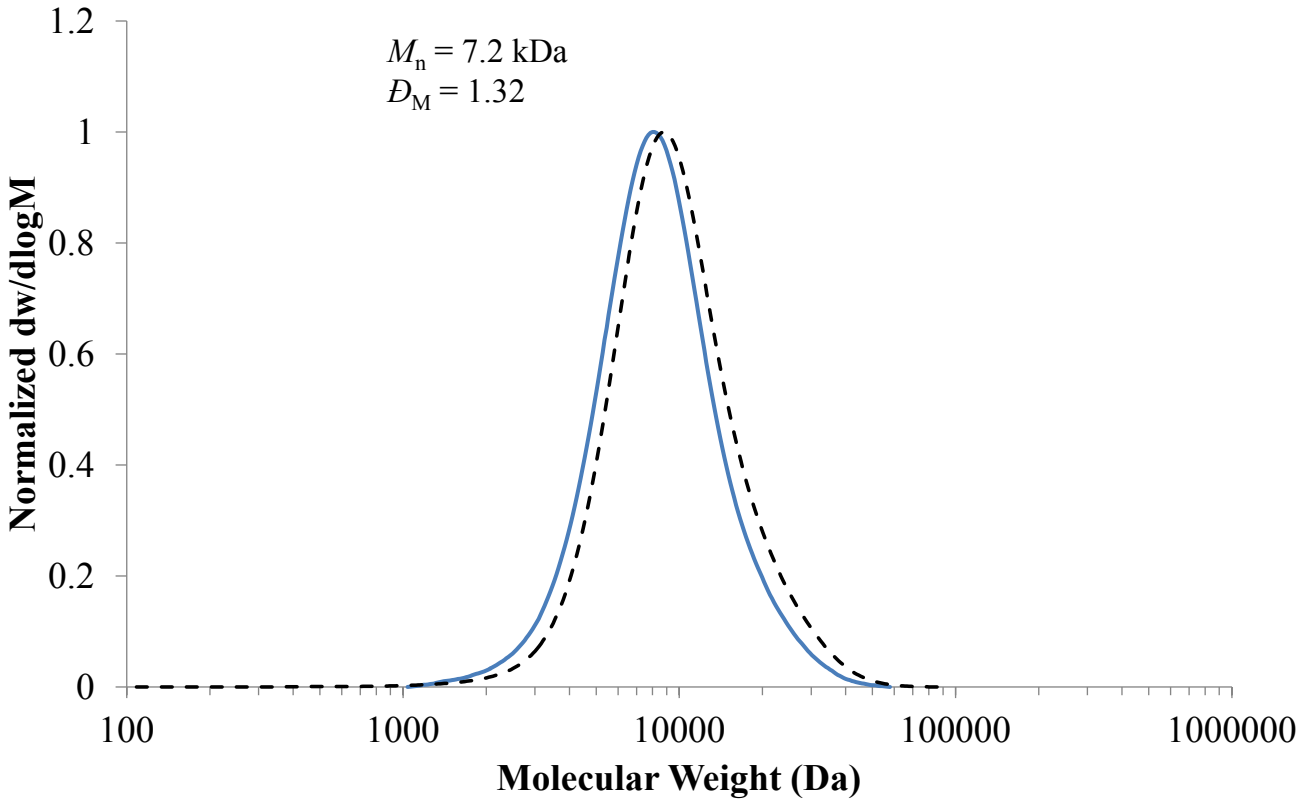

Figure S19 – SEC chromatogram of P($VAc_{0.66}$-co-$MDO_{0.34}$)$_{60}$ formed using **CTA 2** (90 °C, 15 h). Monomer conversion: VAc = 55 %, MDO = 30 %, M_n = 7.2 kDa, $Đ_M$ = 1.32 (SEC $CHCl_3$, based on PS standards). Dashed line indicates the weight distribution obtained from the UV detector @ 280 nm.

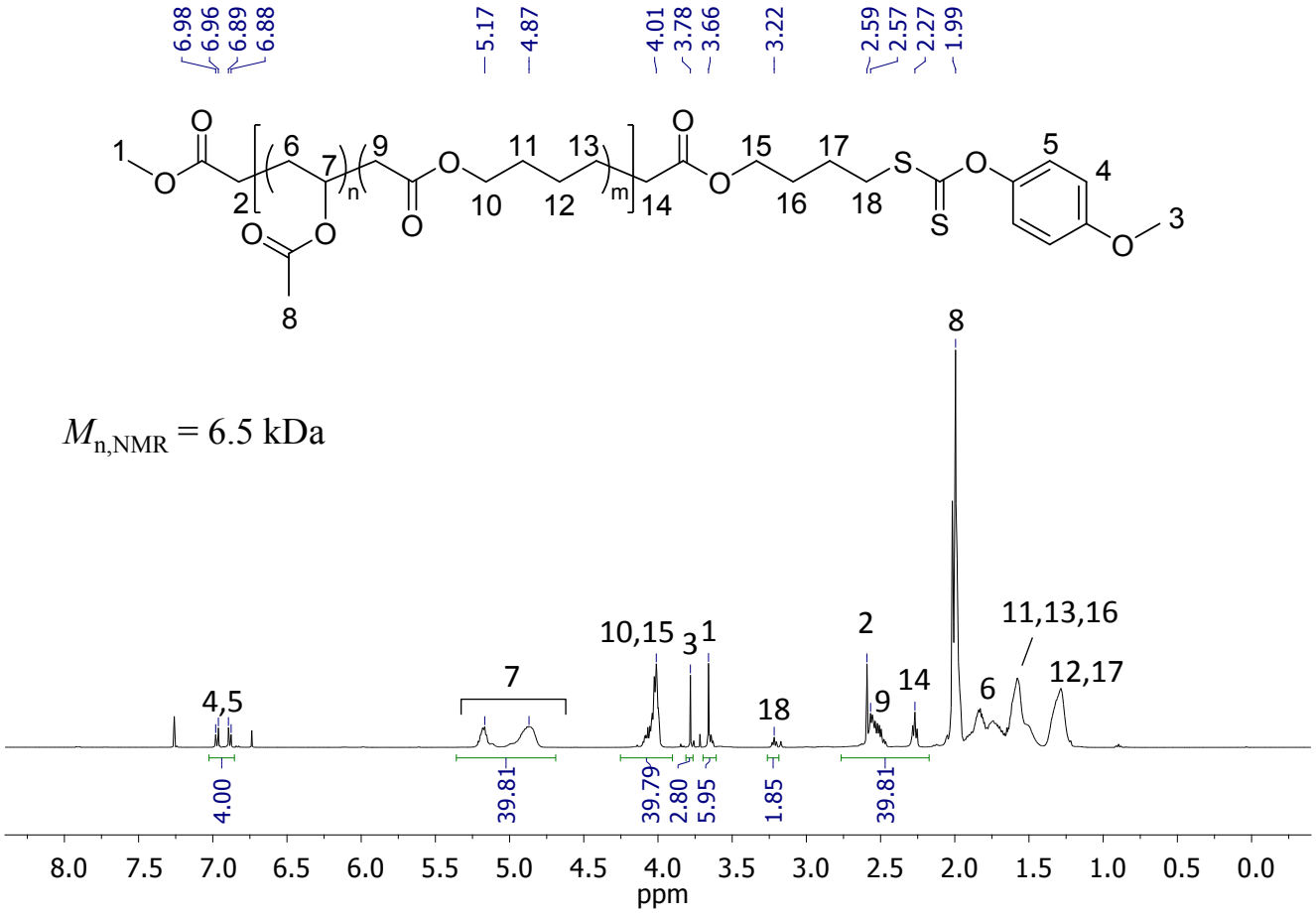

Figure S20 – ^{1}H NMR spectrum of P(VAc$_{0.66}$-co-MDO$_{0.34}$)$_{60}$ formed using **CTA 2** (500 MHz, $CDCl_3$).

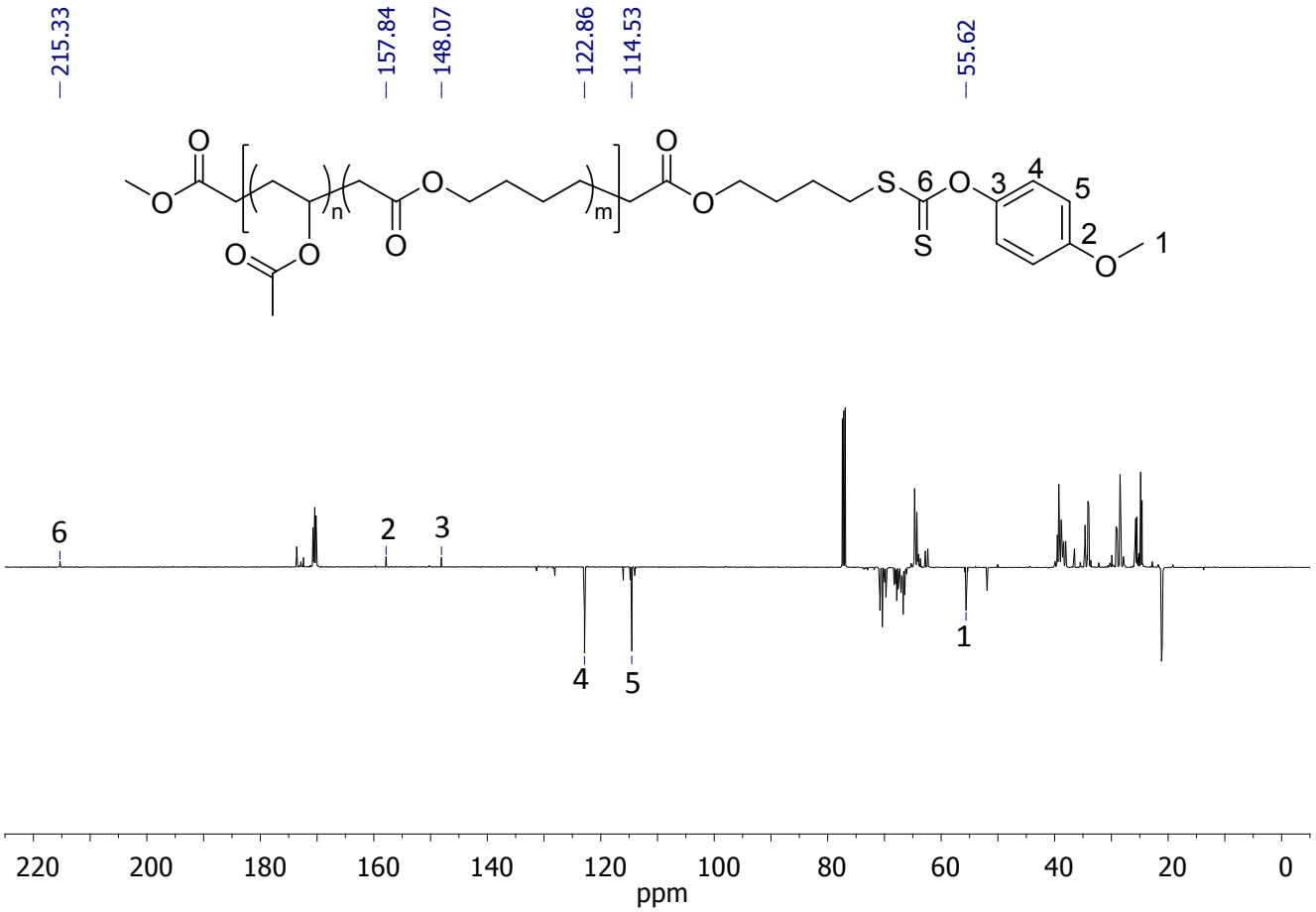

Figure S21 – ^{13}C APT NMR spectrum of $P(VAc_{0.66}\text{-co-}MDO_{0.34})_{60}$ formed using **CTA 2** (125 MHz, $CDCl_3$).

Poly($VAc_{0.46}$-co-$MDO_{0.54}$)$_{50}$ formed using CTA 2

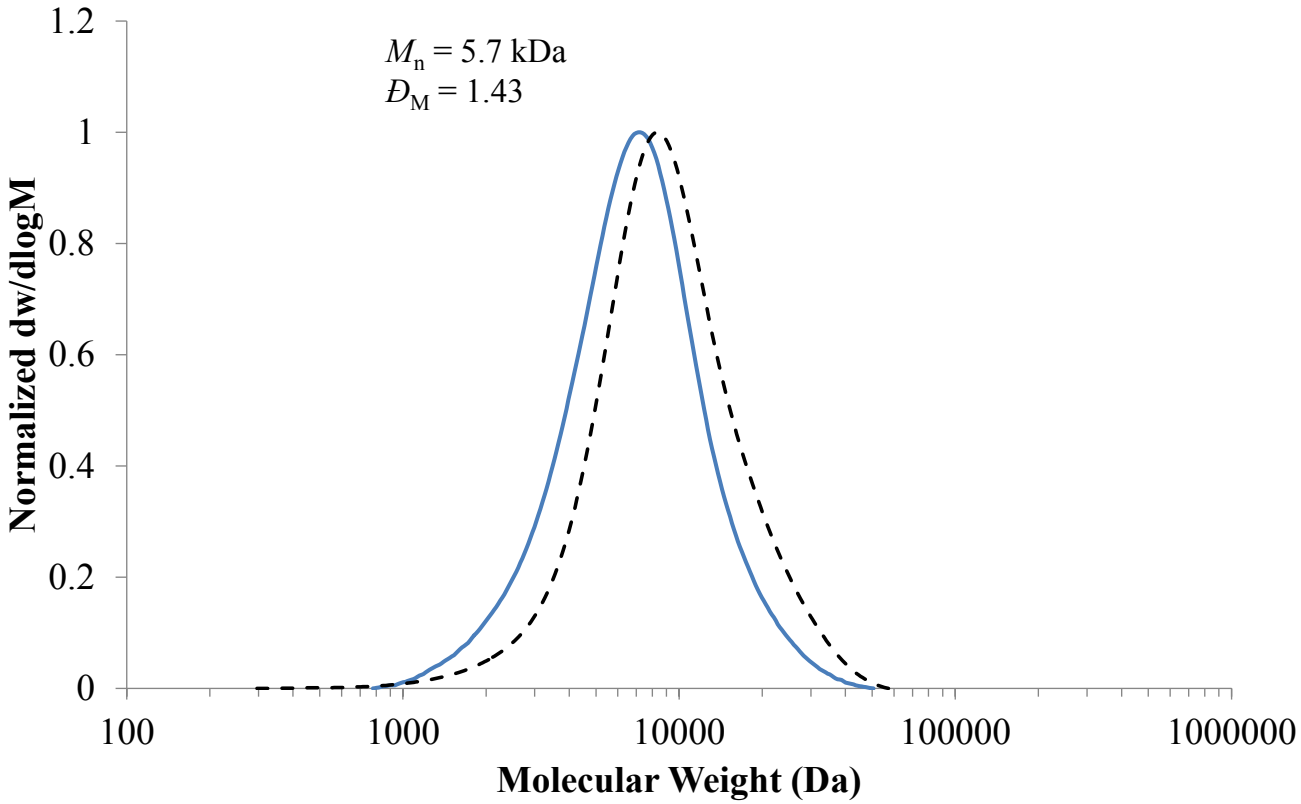

Figure S22 – SEC chromatogram of P($VAc_{0.46}$-co-$MDO_{0.54}$)$_{50}$ formed using **CTA 2** (90 °C, 24 h). Monomer conversion: VAc = 55 %, MDO = 29 %, M_n = 5.7 kDa, $Đ_M$ = 1.43 (SEC $CHCl_3$, based on PS standards). Dashed line indicates the weight distribution obtained from the UV detector @ 280 nm.

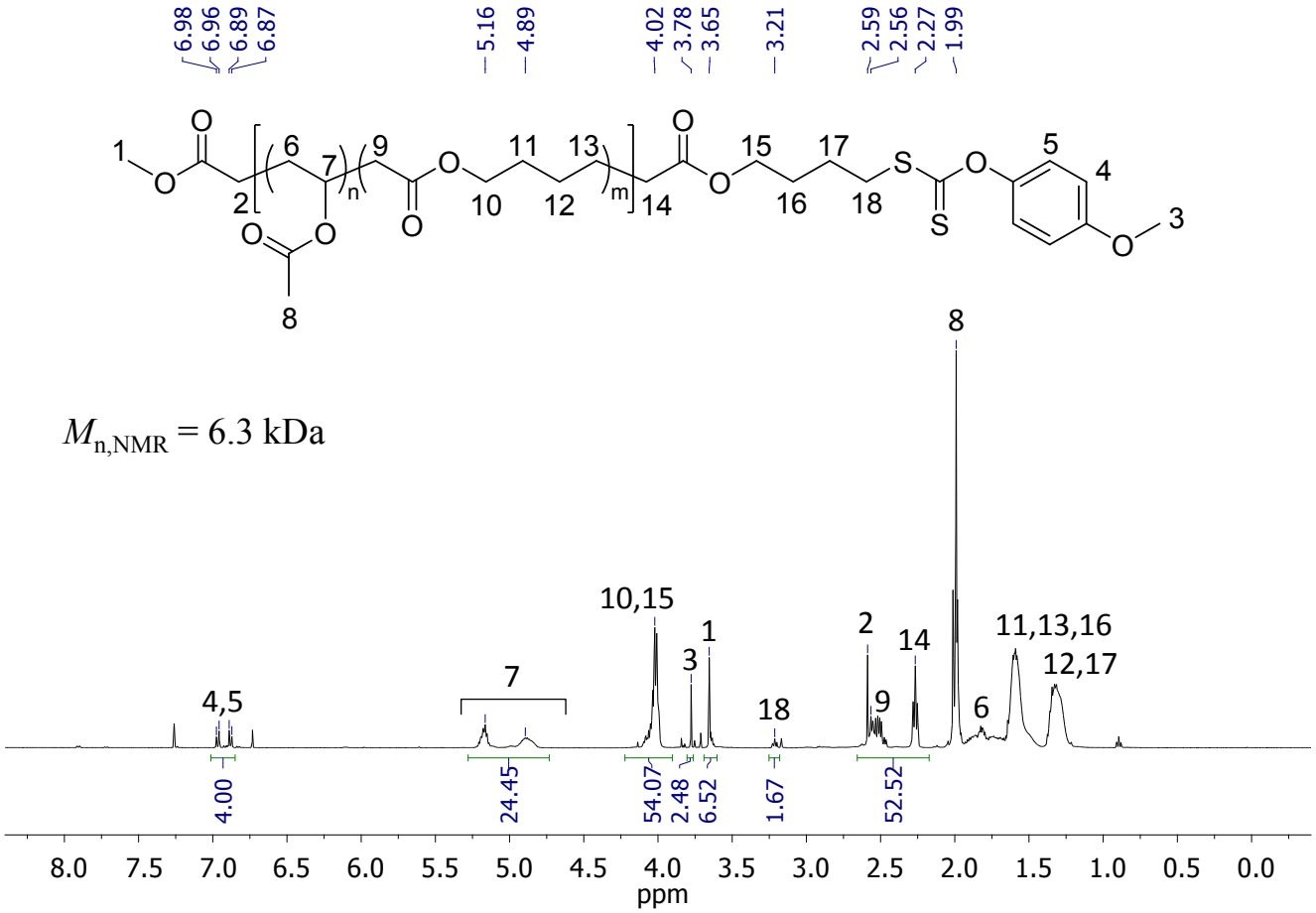

Figure S23 – ^{1}H NMR spectrum of P(VAc$_{0.46}$-co-MDO$_{0.54}$)$_{50}$ formed using **CTA 2** (500 MHz, $CDCl_3$).

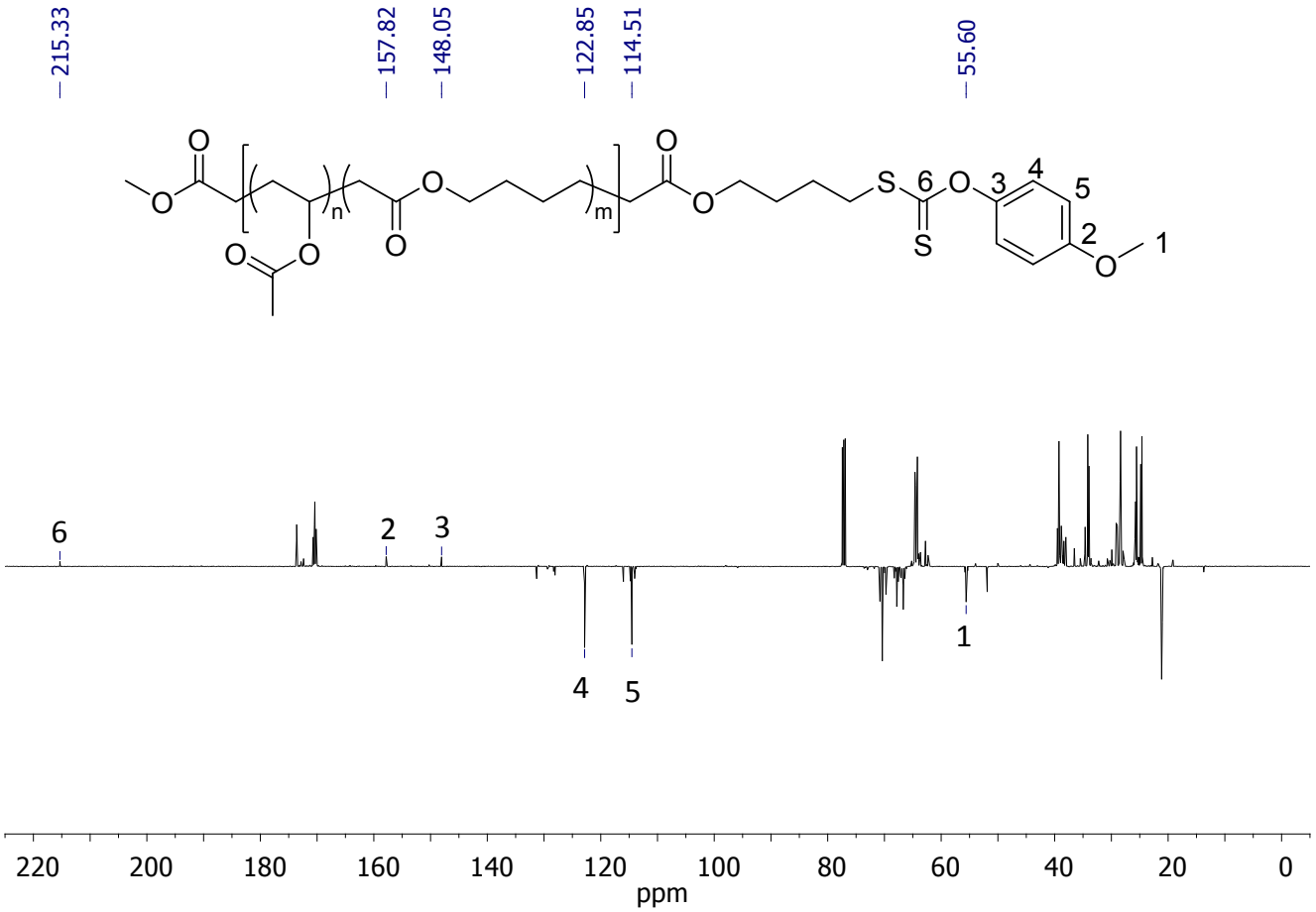

Figure S24 – ^{13}C APT NMR spectrum of $P(VAc_{0.46}\text{-co-}MDO_{0.54})_{50}$ formed using **CTA 2** (125 MHz, $CDCl_3$).

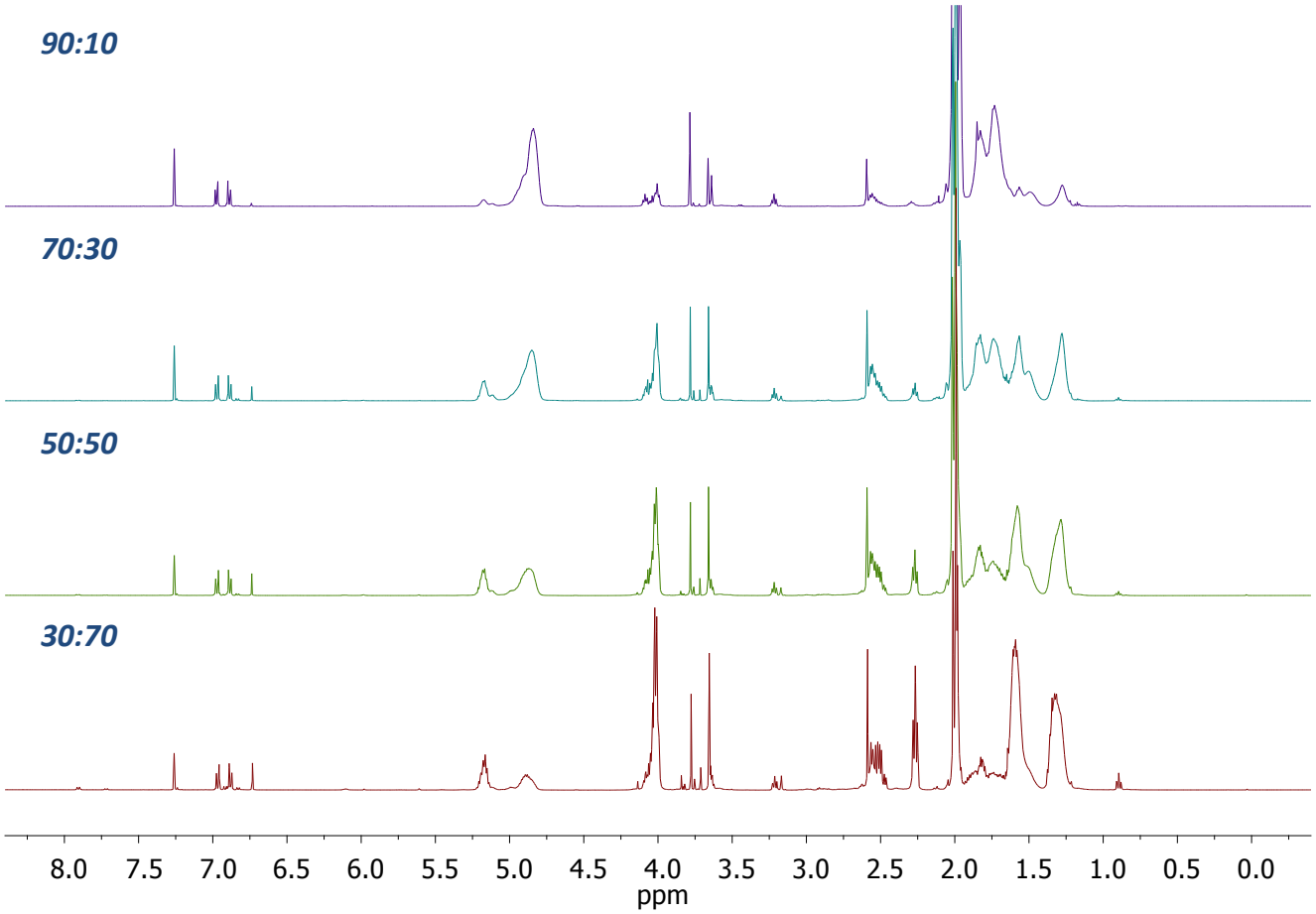

Figure S25 – ^{1}H NMR spectral comparison of all copolymers of P(VAc-co-MDO) using **CTA 2** (500 MHz, $CDCl_3$).

Poly(MDO)$_{29}$ formed using CTA 2

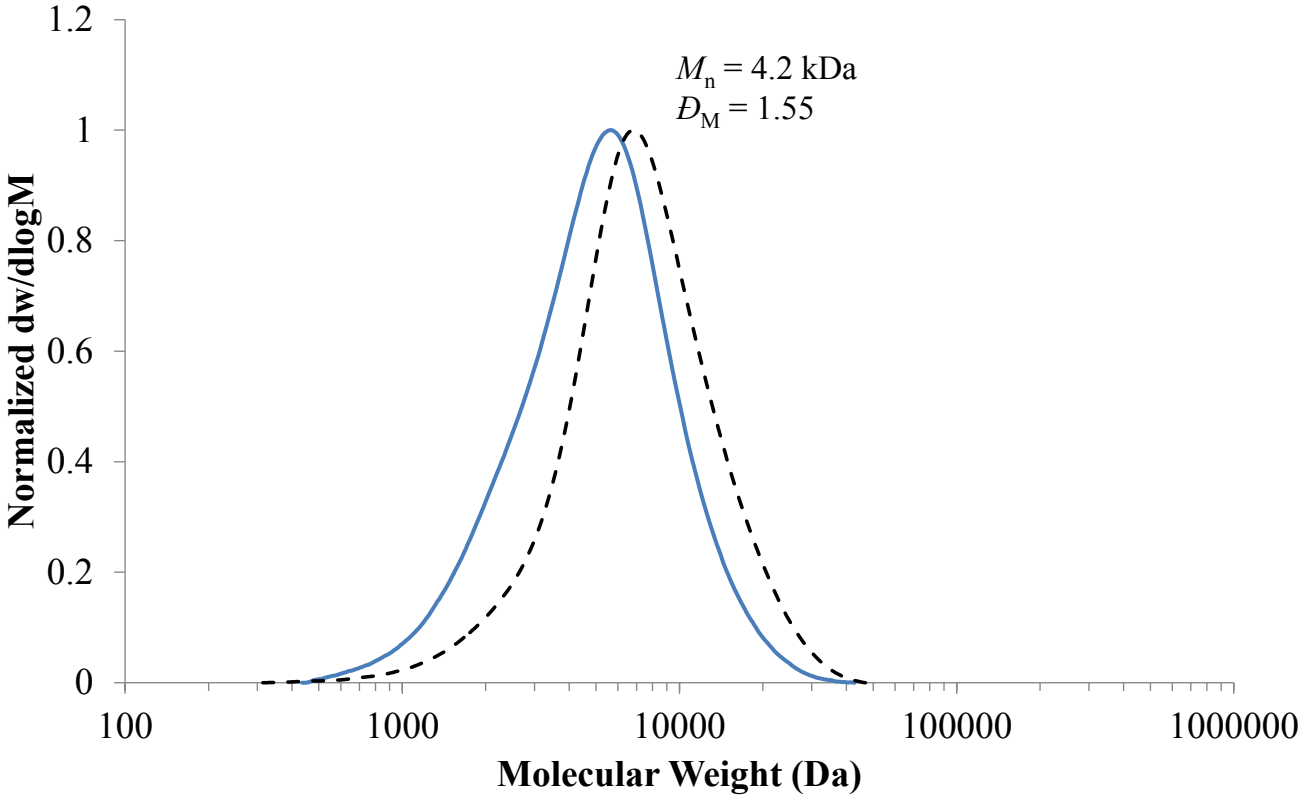

Figure S26 – SEC chromatogram of poly(MDO)$_{29}$ formed using **CTA 2** (90 °C, 24 h). Monomer conversion = 22 %, M_n = 4.2 kDa, $Đ_M$ = 1.55 (SEC $CHCl_3$, based on PS standards). Dashed line indicates the weight distribution obtained from the UV detector @ 280 nm.

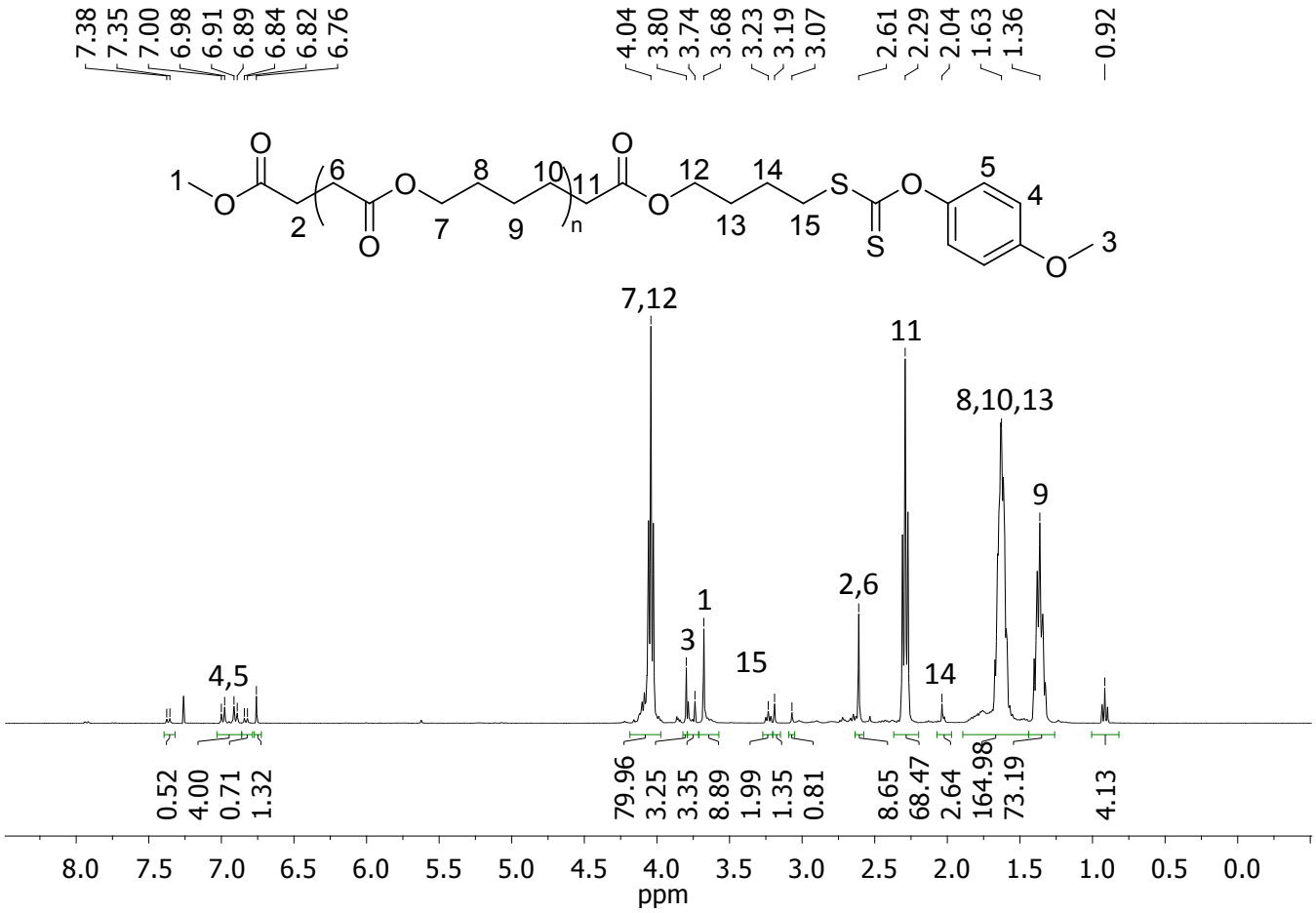

Figure S27 – ^{1}H NMR spectrum of poly(MDO)$_{29}$ formed using **CTA 2** (500 MHz, $CDCl_3$).

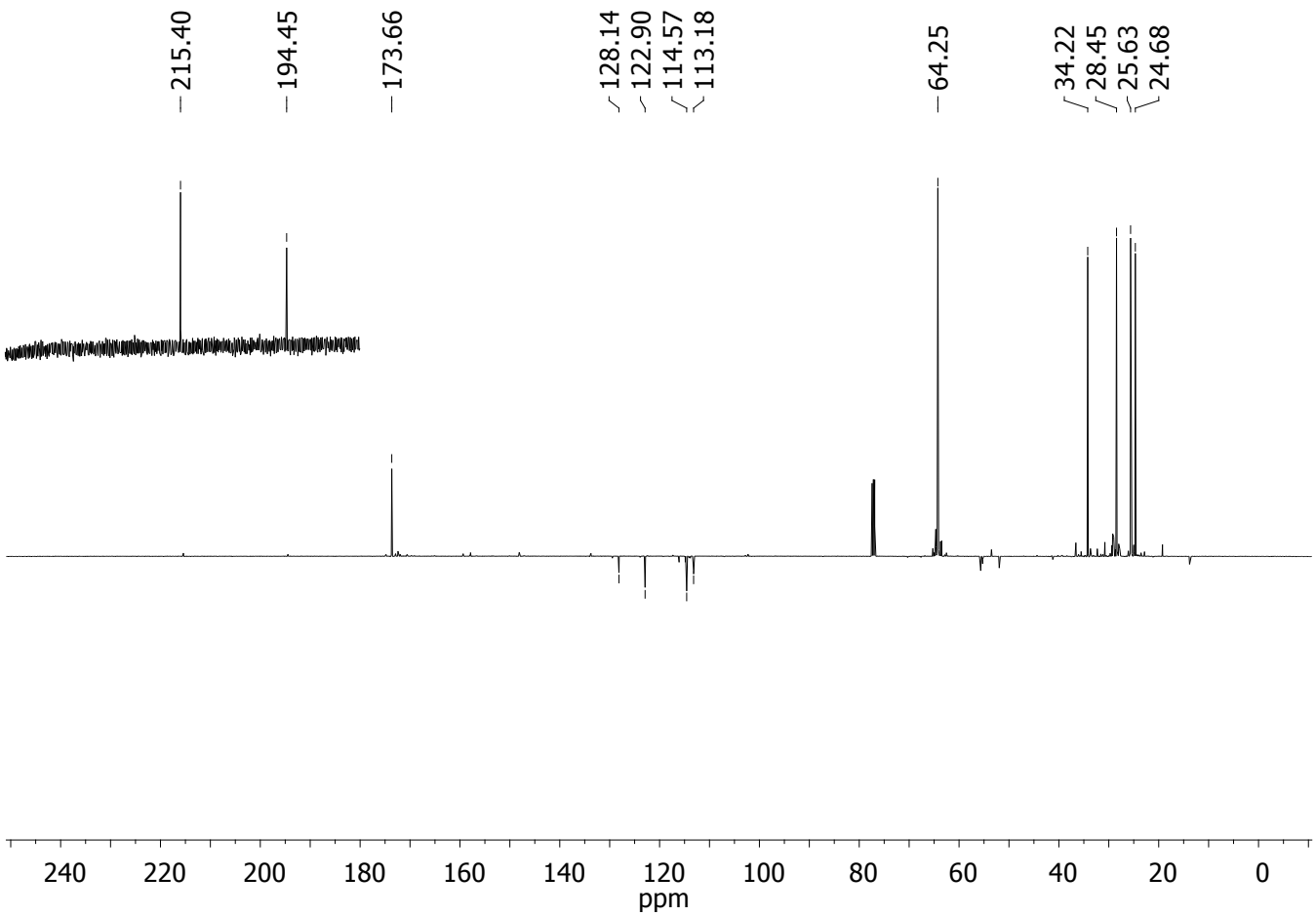

Figure S28 – ^{13}C APT NMR spectrum of poly(MDO)$_{29}$ formed using **CTA 2** (125 MHz, $CDCl_3$).

Poly(MDO)$_{29}$ formed using CTA 1

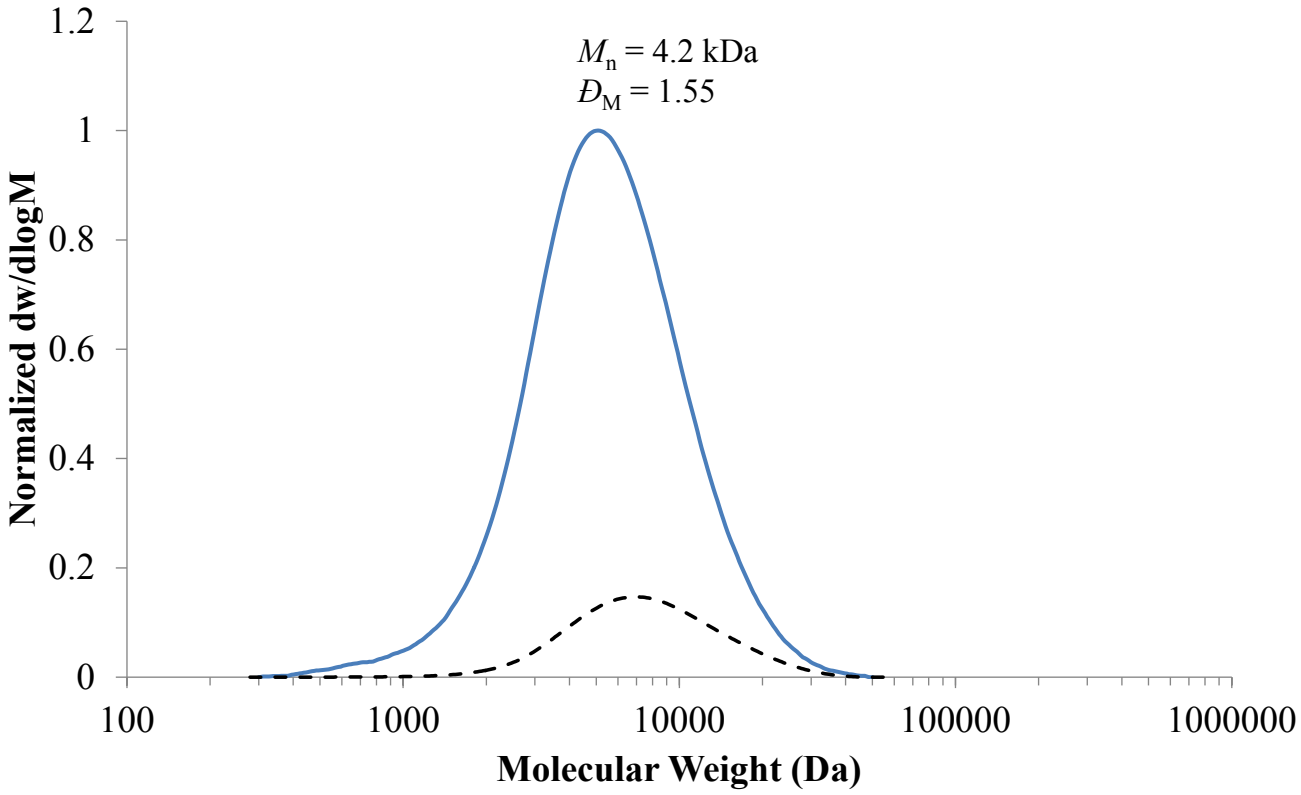

Figure S29 – SEC chromatogram of poly(MDO)$_{29}$ formed using CTA **1** (60 °C, 24 h). Monomer conversion = 20 %, M_n = 4.2 kDa, $Đ_M$ = 1.55 (SEC $CHCl_3$, based on PS standards). Dashed line (---): UV trace @ 280 nm (normalized to RI signal).

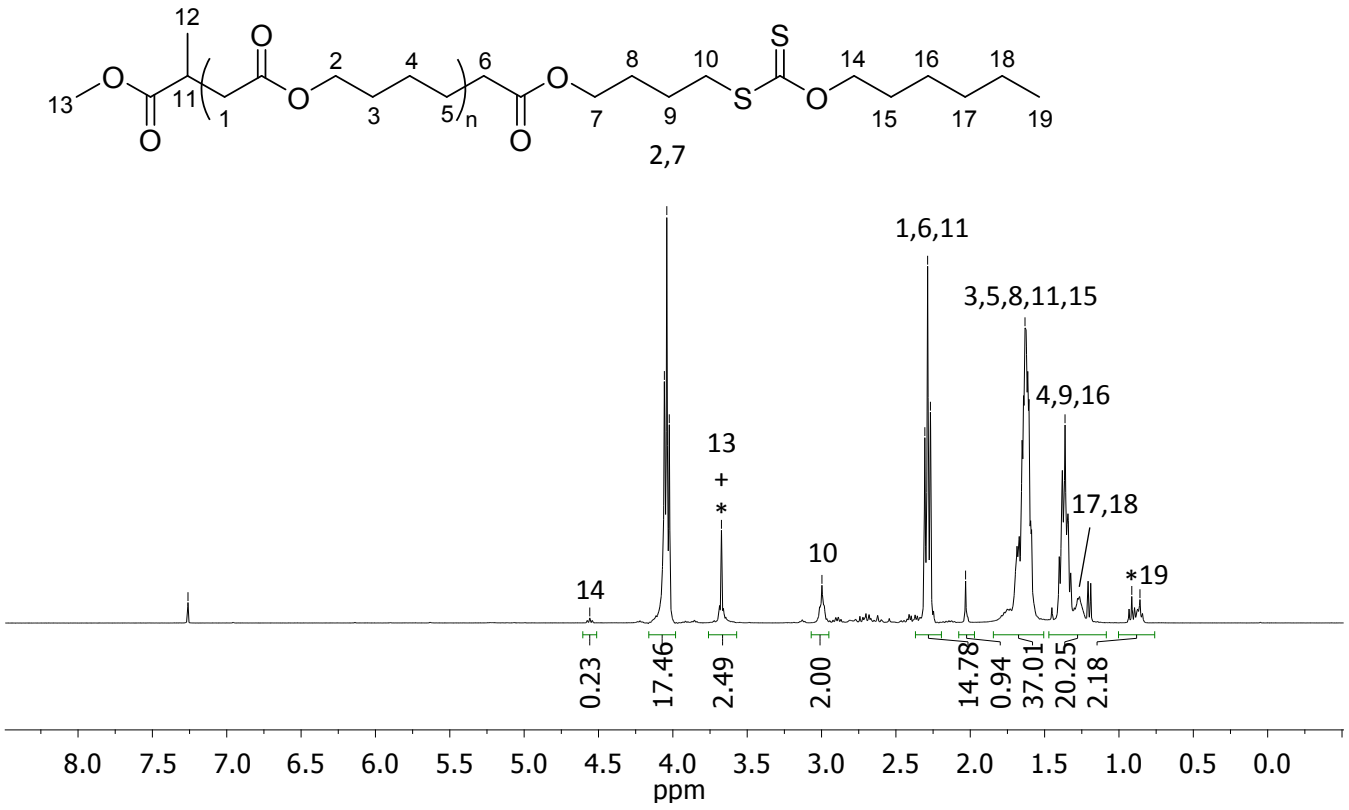

Figure S30 – ^{1}H NMR spectrum of poly(MDO)$_{29}$ formed using CTA **1** (500 MHz, $CDCl_3$). * 1,4- and 1,7-H abstraction side reactions.

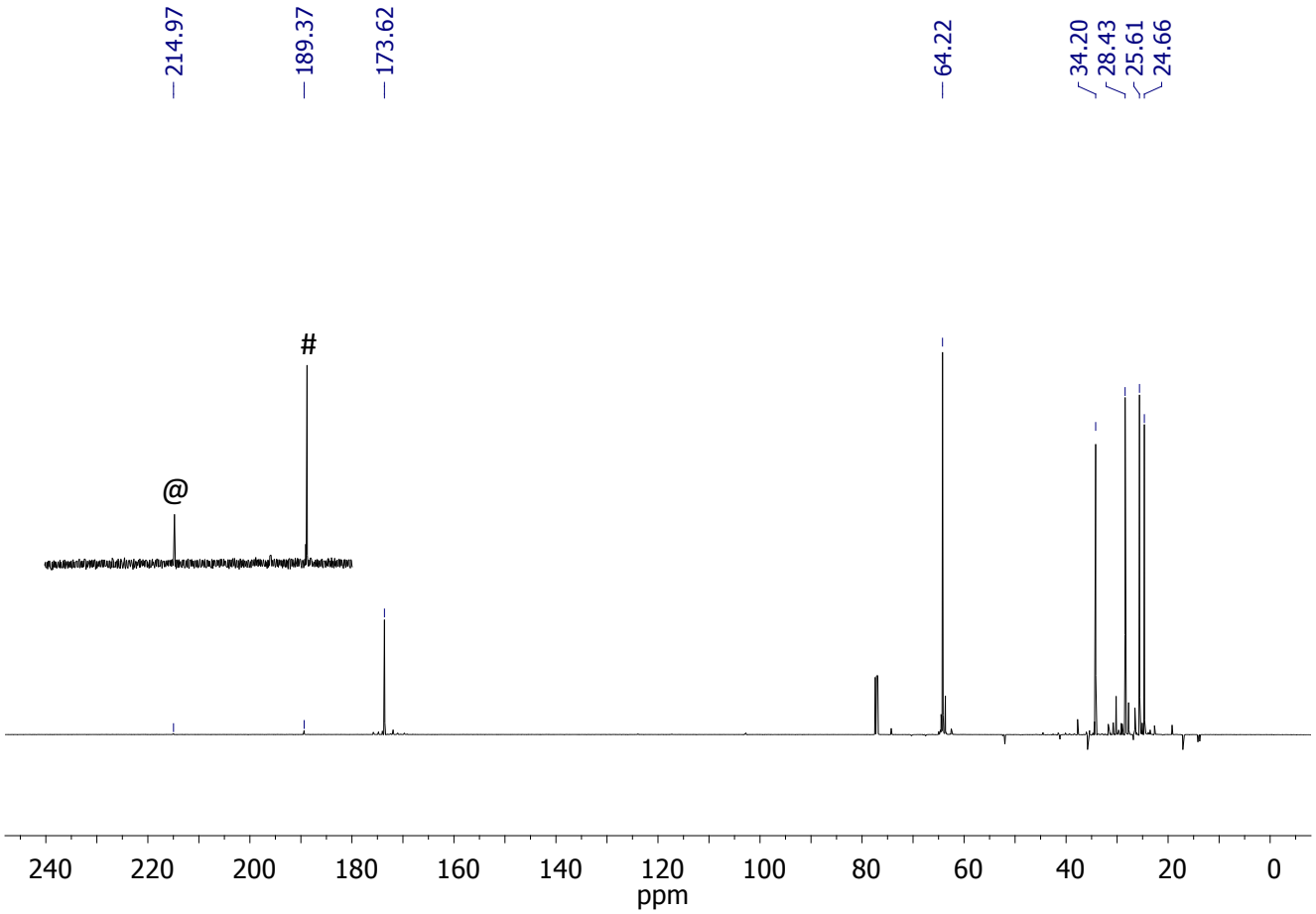

Figure S31 – ^{13}C APT NMR spectrum of poly(MDO)$_{29}$ formed using CTA **1** (125 MHz, $CDCl_3$). Insert: expanded section from δ =]180 – 240 ppm showing: @ - Peak associated with xanthate; # - Peak associated with the carbonodithioate carbonyl.

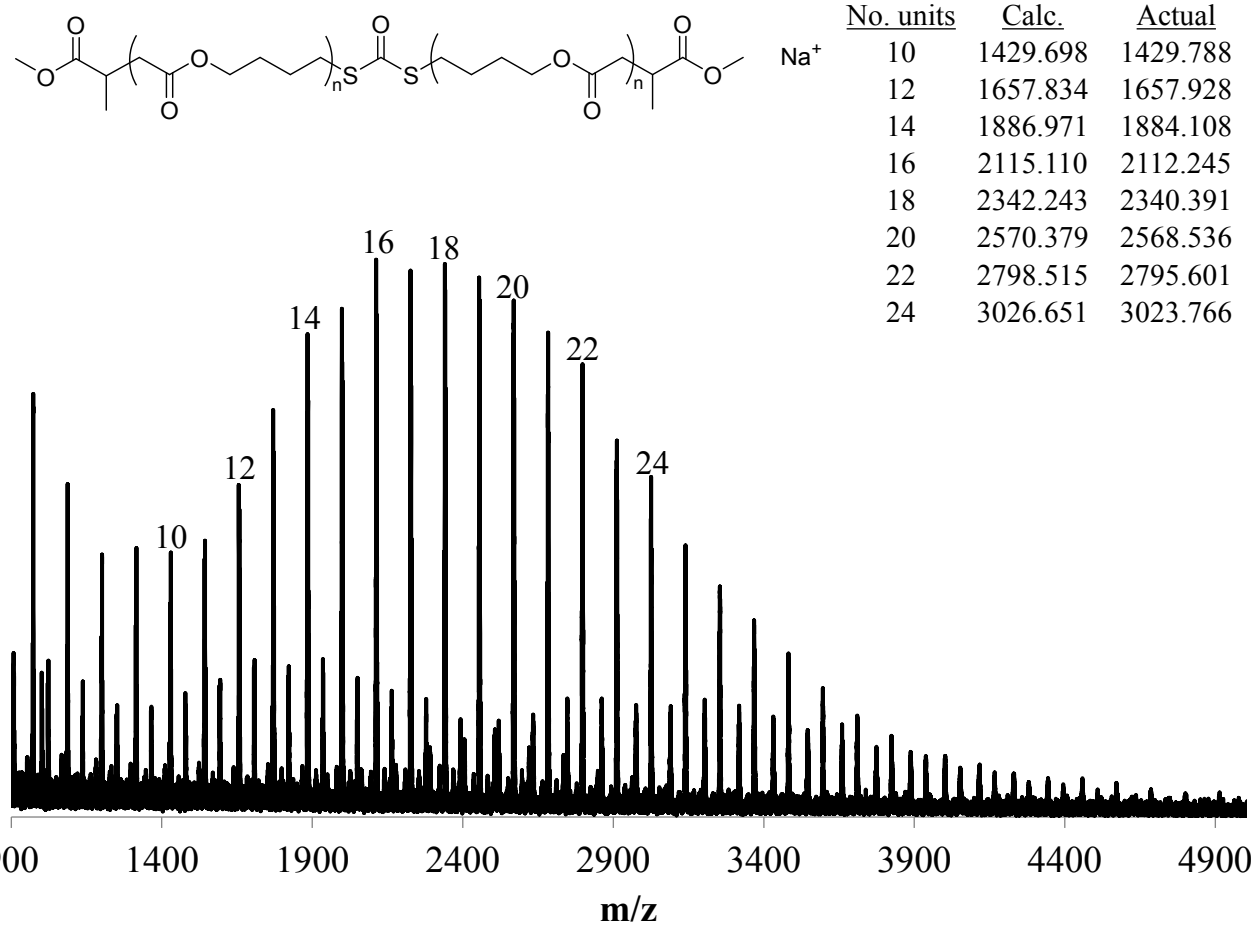

No. units	Calc.	Actual
10	1429.698	1429.788
12	1657.834	1657.928
14	1886.971	1884.108
16	2115.110	2112.245
18	2342.243	2340.391
20	2570.379	2568.536
22	2798.515	2795.601
24	3026.651	3023.766

Figure S32 – MALDI-ToF mass spectrum of poly(MDO)$_{29}$ formed using **CTA 1** (60 °C, 24 h).

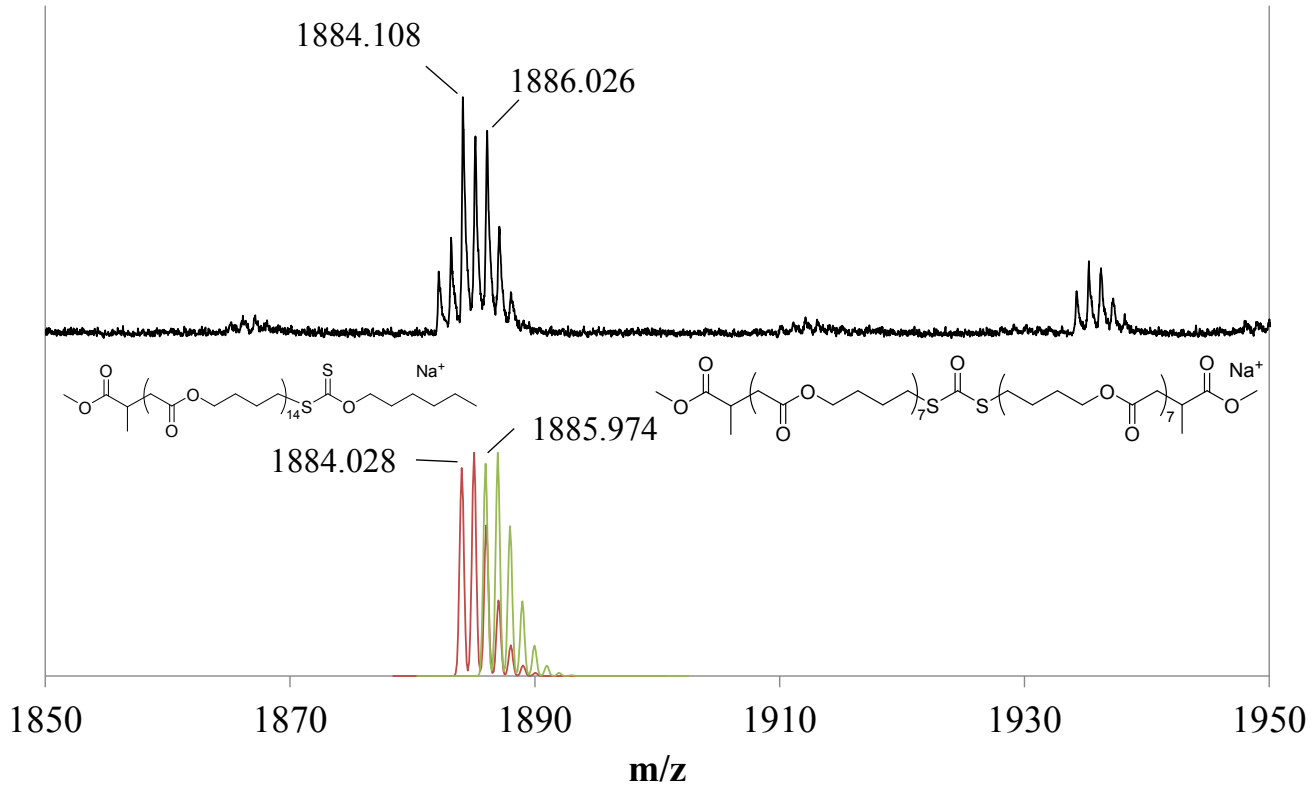

Figure S33 – MALDI-ToF MS isotopic distribution of poly(MDO)$_{14}$ formed using **CTA 1** (60 °C, 24 h). Top = measured, bottom = simulated.

Poly(MDO)$_{14}$ formed using CTA 2

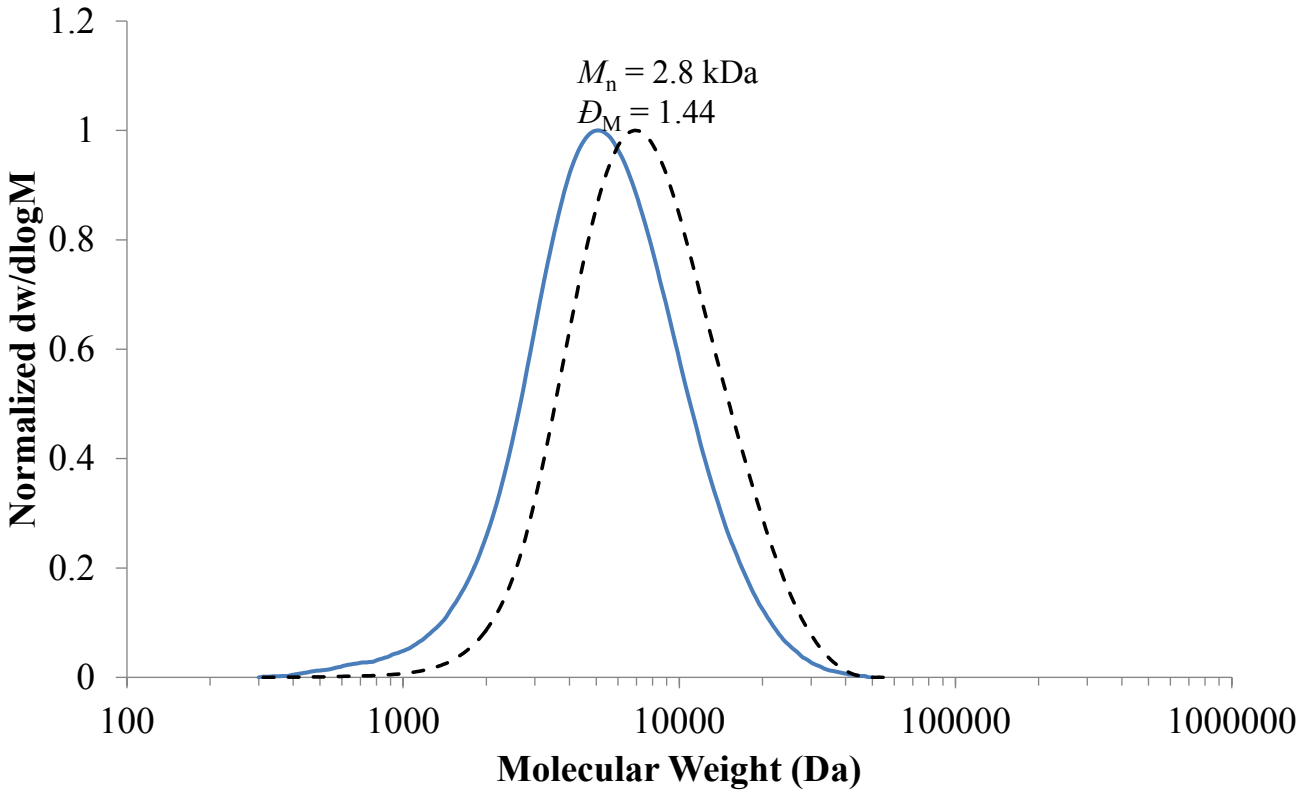

Figure S34 – SEC chromatogram of poly(MDO)$_{14}$ formed using **CTA 2** (90 °C, 24 h). Monomer conversion = 15 %, M_n = 2.4 kDa, $Đ_M$ = 1.41 (SEC $CHCl_3$, based on PS standards). Dashed line indicates the weight distribution obtained from the UV detector @ 280 nm.

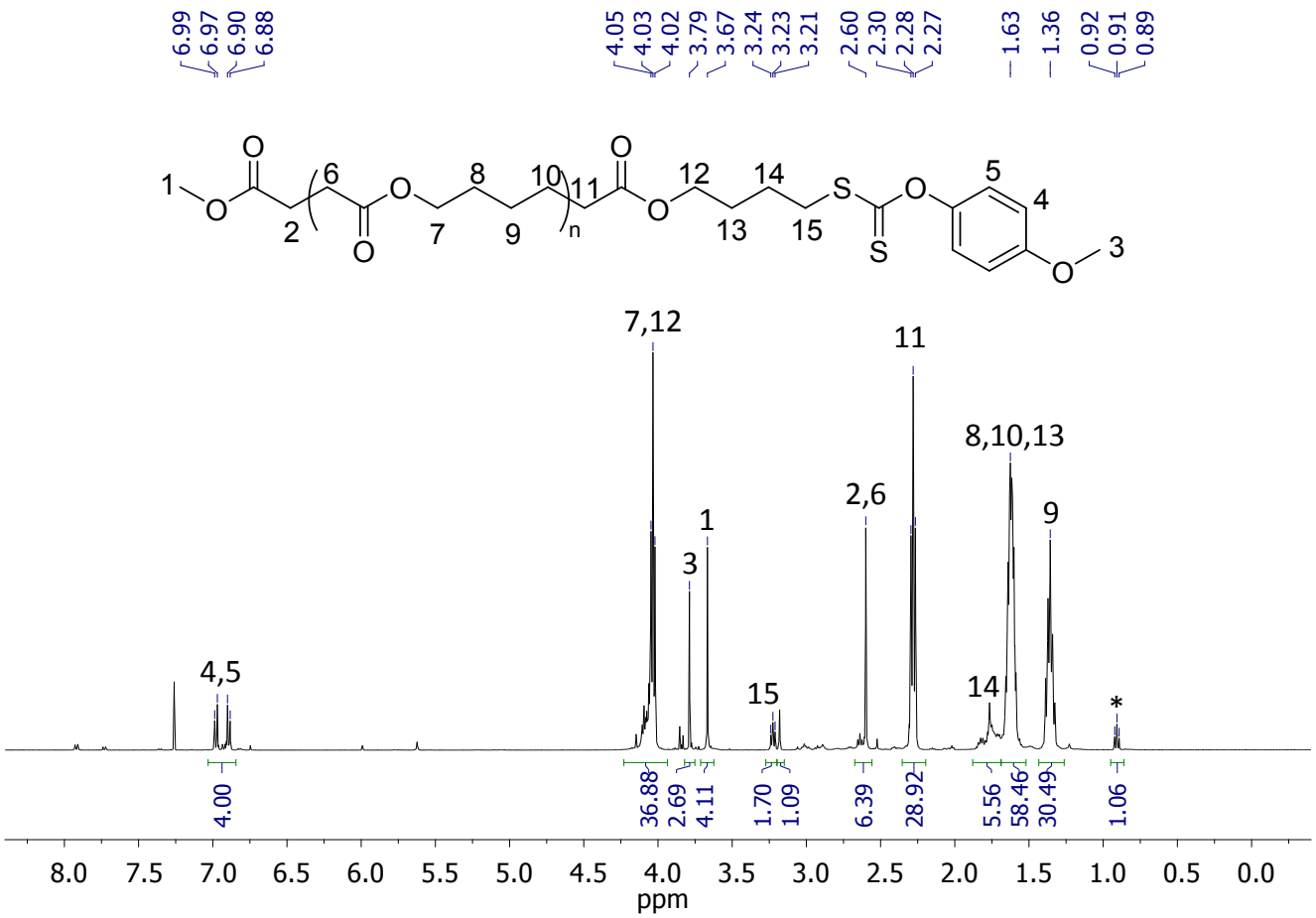

Figure S35 – ^{1}H NMR spectrum of poly(MDO)$_{14}$ formed using **CTA 2** (500 MHz, $CDCl_3$). * 1,4- and 1,7-H abstraction side reactions.

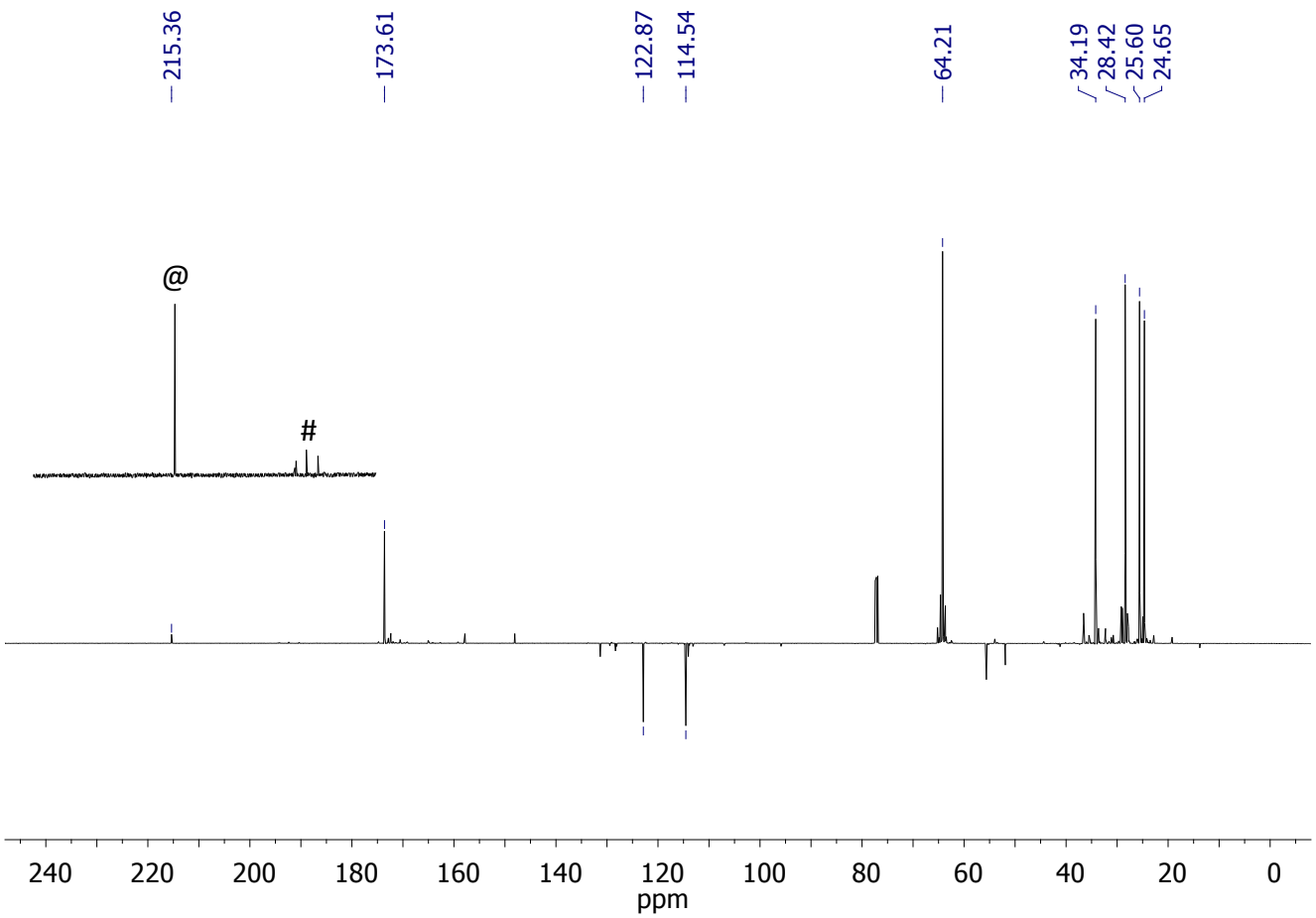

Figure S36 – ^{13}C APT NMR spectrum of poly(MDO)$_{14}$ formed using **CTA 2** (125 MHz, $CDCl_3$). Insert: expanded section from δ = 180 – 240 ppm showing: @ - Peak associated with xanthate; # - Peak associated with the carbonodithioate carbonyl.

Figure S37 – MALDI-ToF mass spectrum of poly(MDO)$_{14}$ formed using **CTA 2** (90 °C, 24 h). Smaller distribution attributed to azo initiated polymer chains and H-abstraction side reactions.

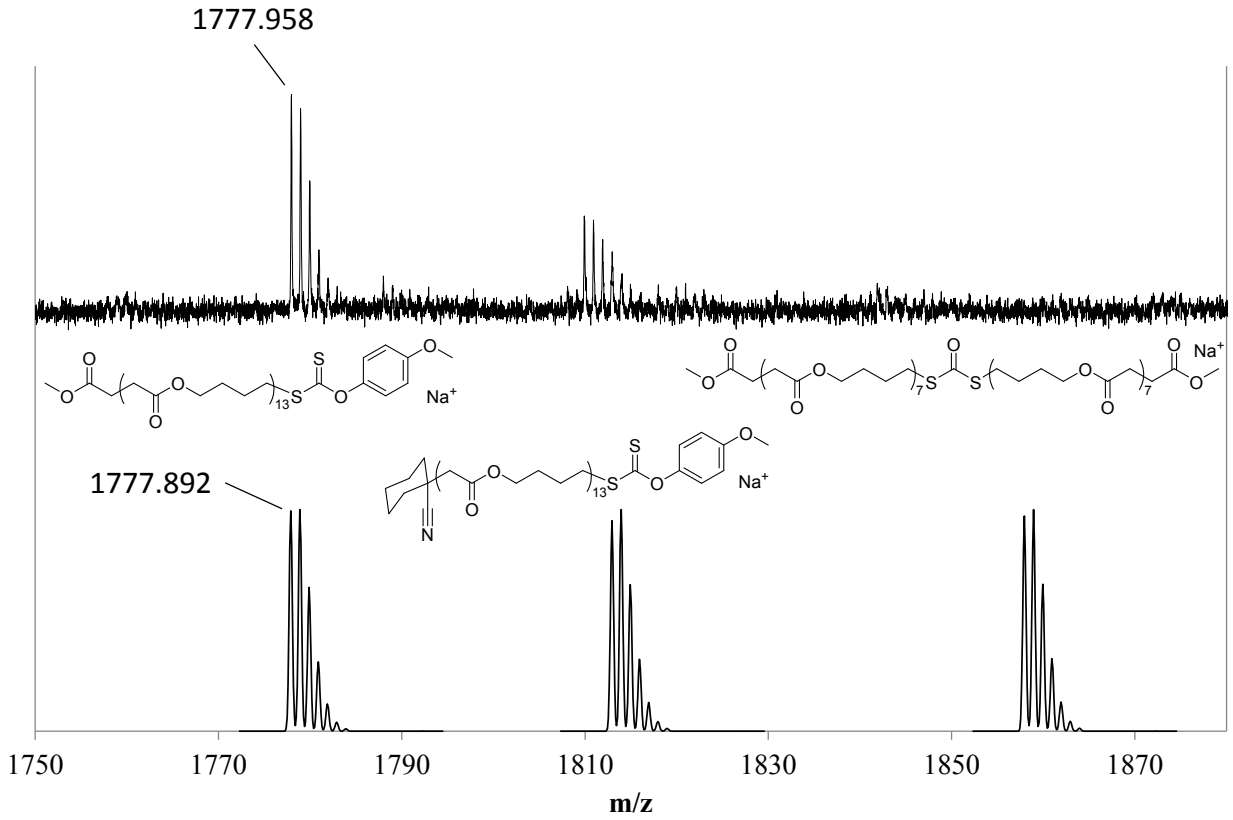

Figure S38 – MALDI-ToF MS isotopic distribution of poly(MDO)$_{14}$ formed using **CTA 2** (90 °C, 24 h). Top = measured, bottom = simulated.

Poly(MDO)$_{25}$ formed using CTA 3

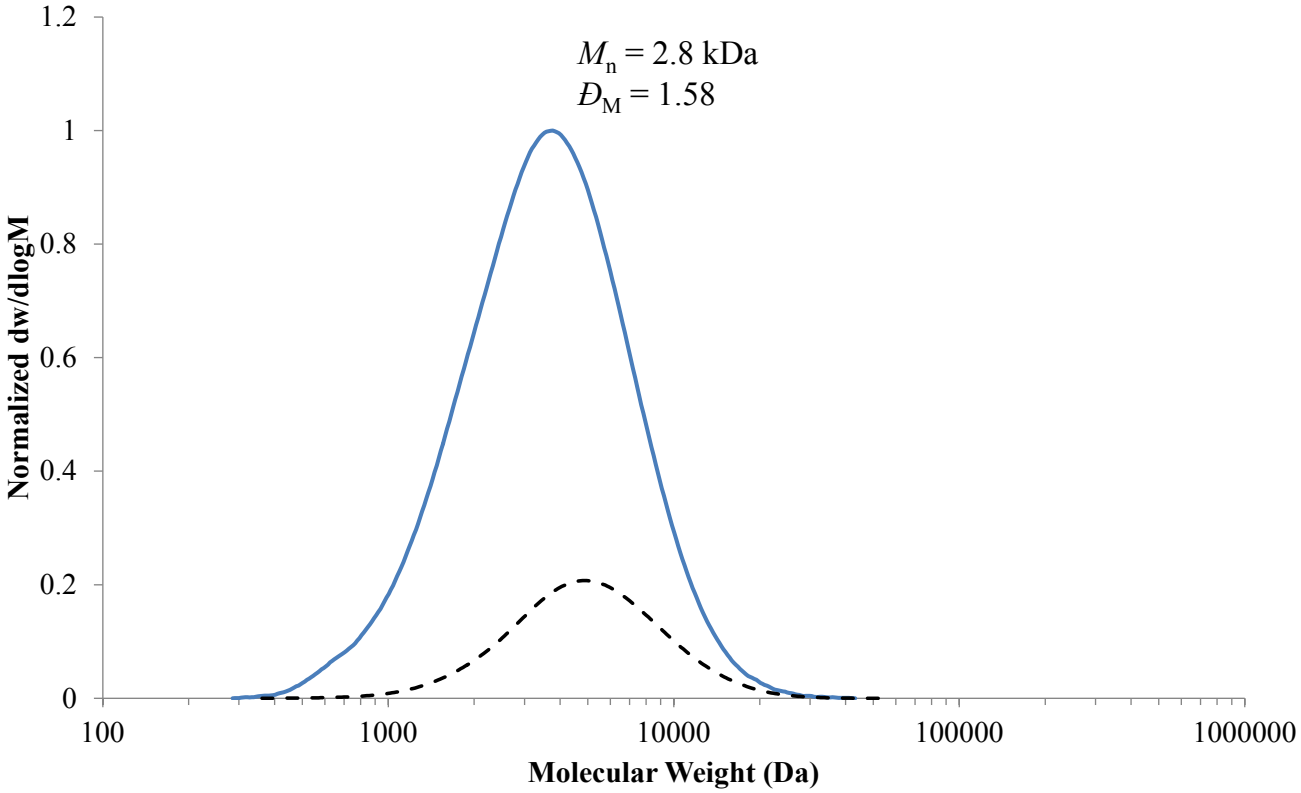

Figure S39 – SEC chromatogram of poly(MDO)$_{25}$ formed using CTA **3** (60 °C, 24 h). Monomer conversion = 22 %, M_n = 2.8 kDa, $Đ_M$ = 1.58 (SEC $CHCl_3$, based on PS standards). Dashed line (---): UV trace @ 280 nm (normalized to RI signal).

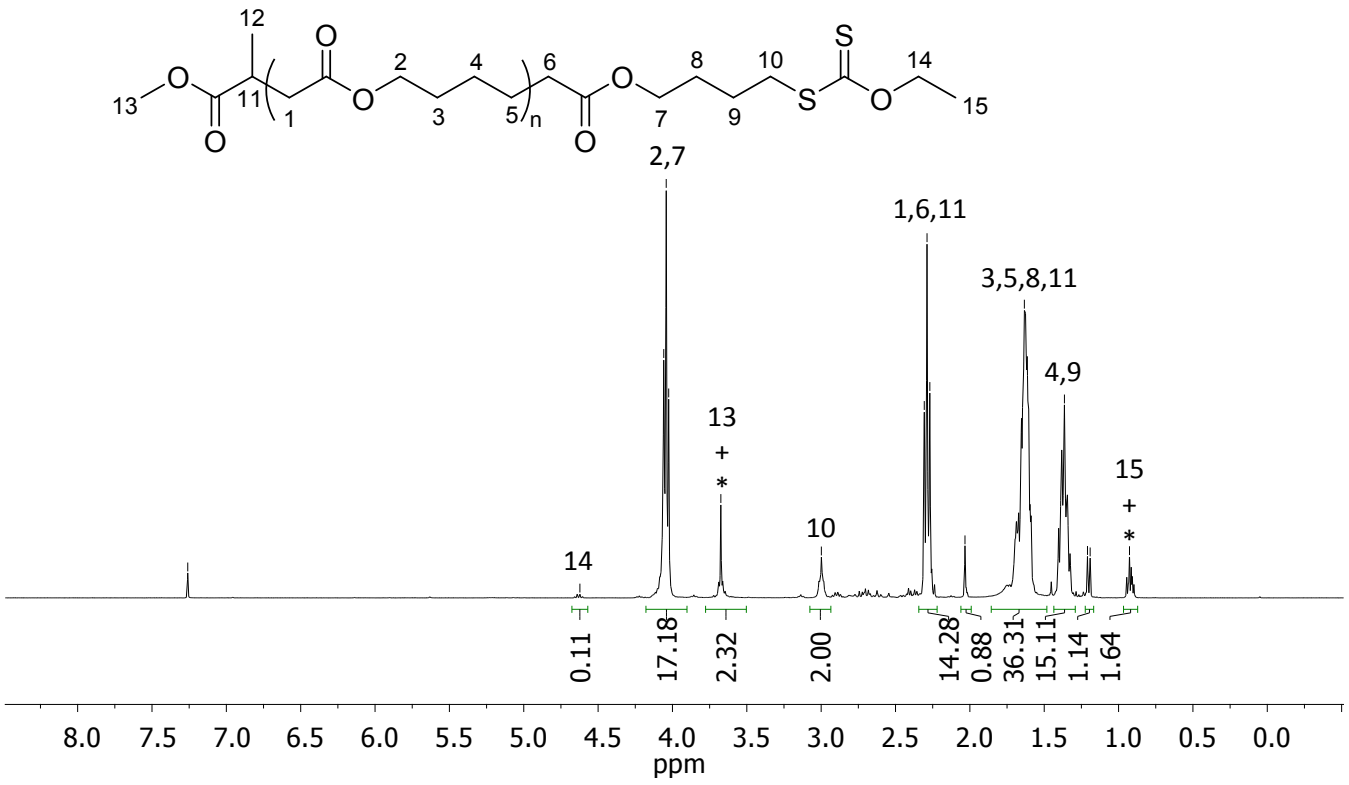

Figure S40 – ^{1}H NMR spectrum of poly(MDO)$_{25}$ formed using CTA **3** (500 MHz, $CDCl_3$). * 1,4- and 1,7-H abstraction side reactions.

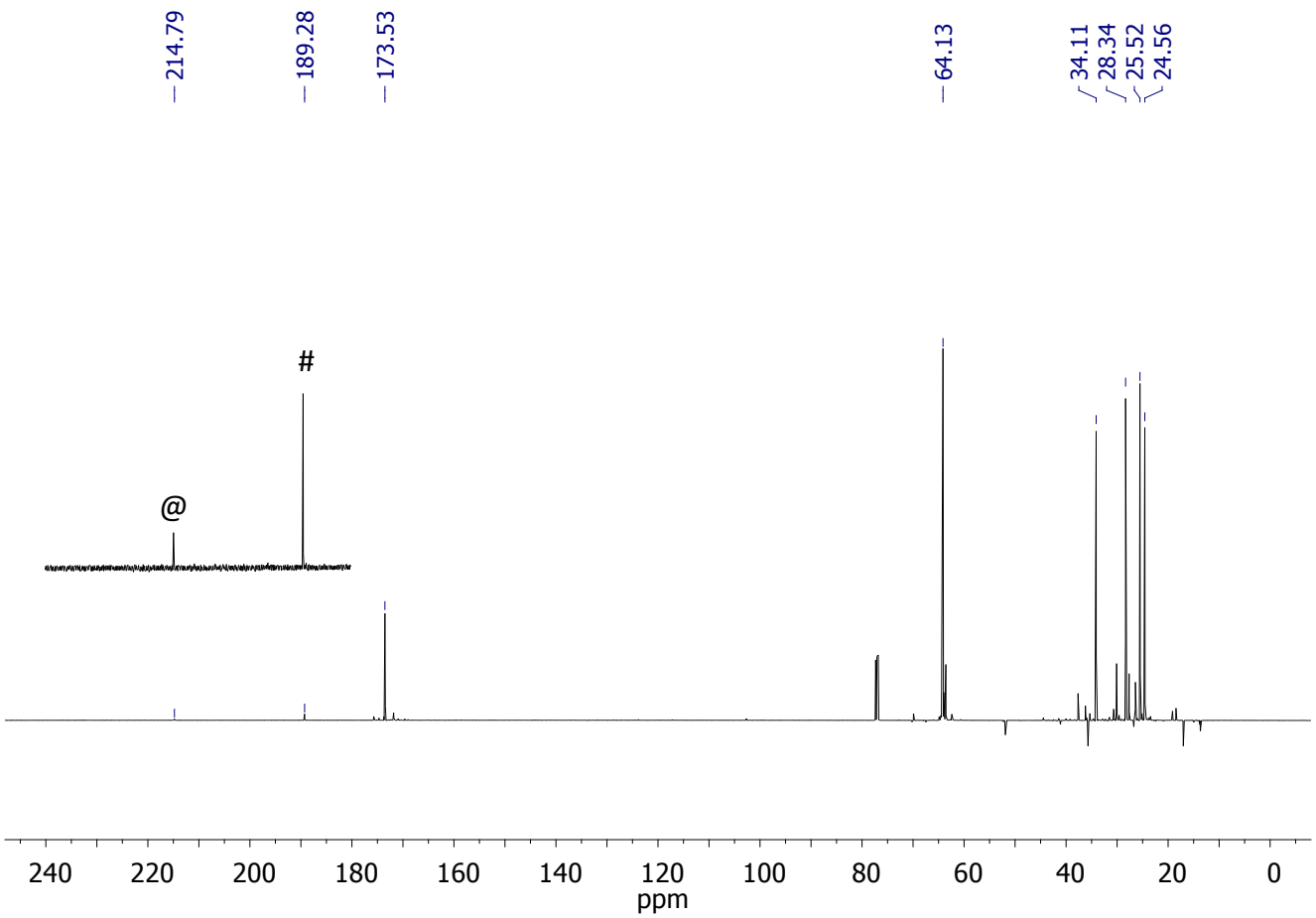

Figure S41 – ^{13}C APT NMR spectrum of poly(MDO)$_{25}$ formed using CTA **3** (125 MHz, $CDCl_3$). Insert: expanded section from δ = 180 – 240 ppm showing: @ - Peak associated with the xanthate; # - Peak associated with the carbonodithioate carbonyl.

Poly(MDO)$_{34}$ formed using CTA 4

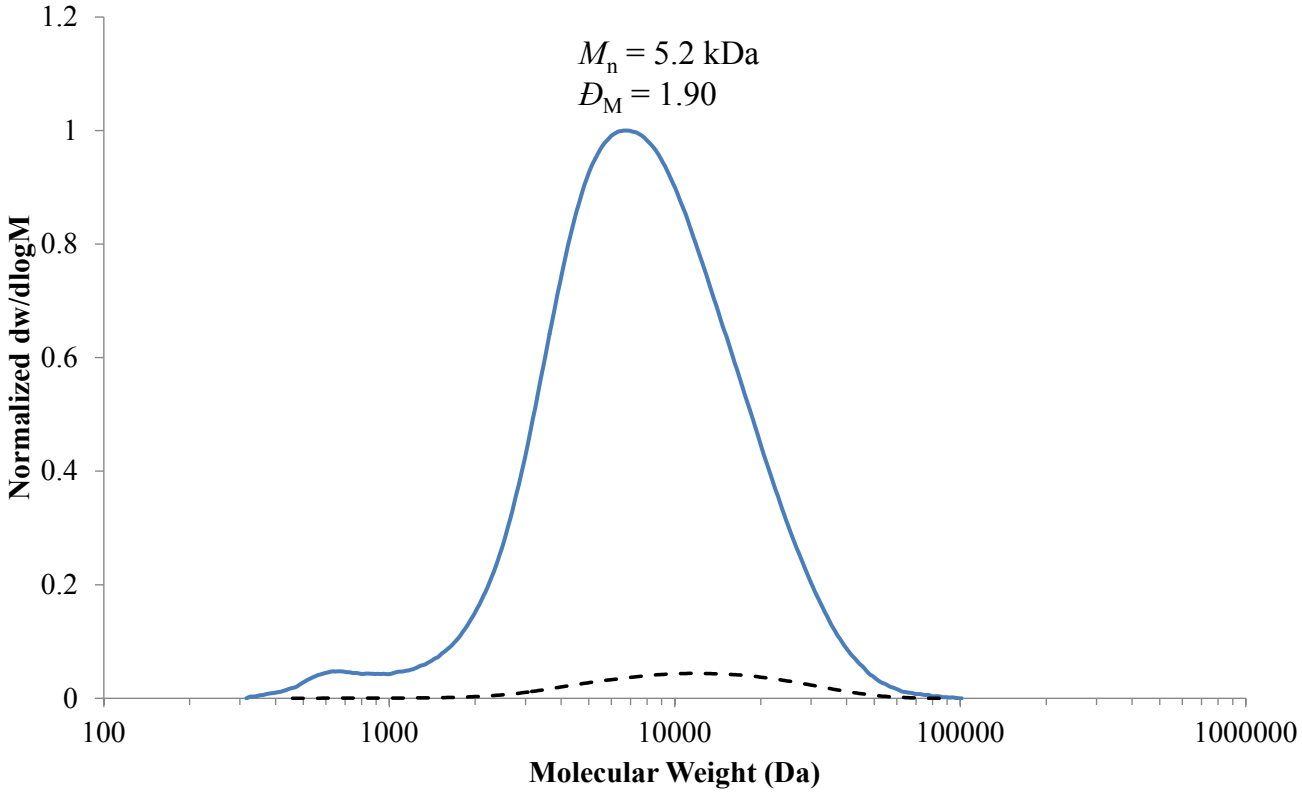

Figure S42 – SEC chromatogram of poly(MDO)$_{34}$ formed using CTA **4** (60 °C, 24 h). Monomer conversion = 21%, M_n = 5.2 kDa, $Đ_M$ = 1.90 (SEC $CHCl_3$, based on PS standards). Dashed line (---): UV trace @ 280 nm (normalized to RI signal).

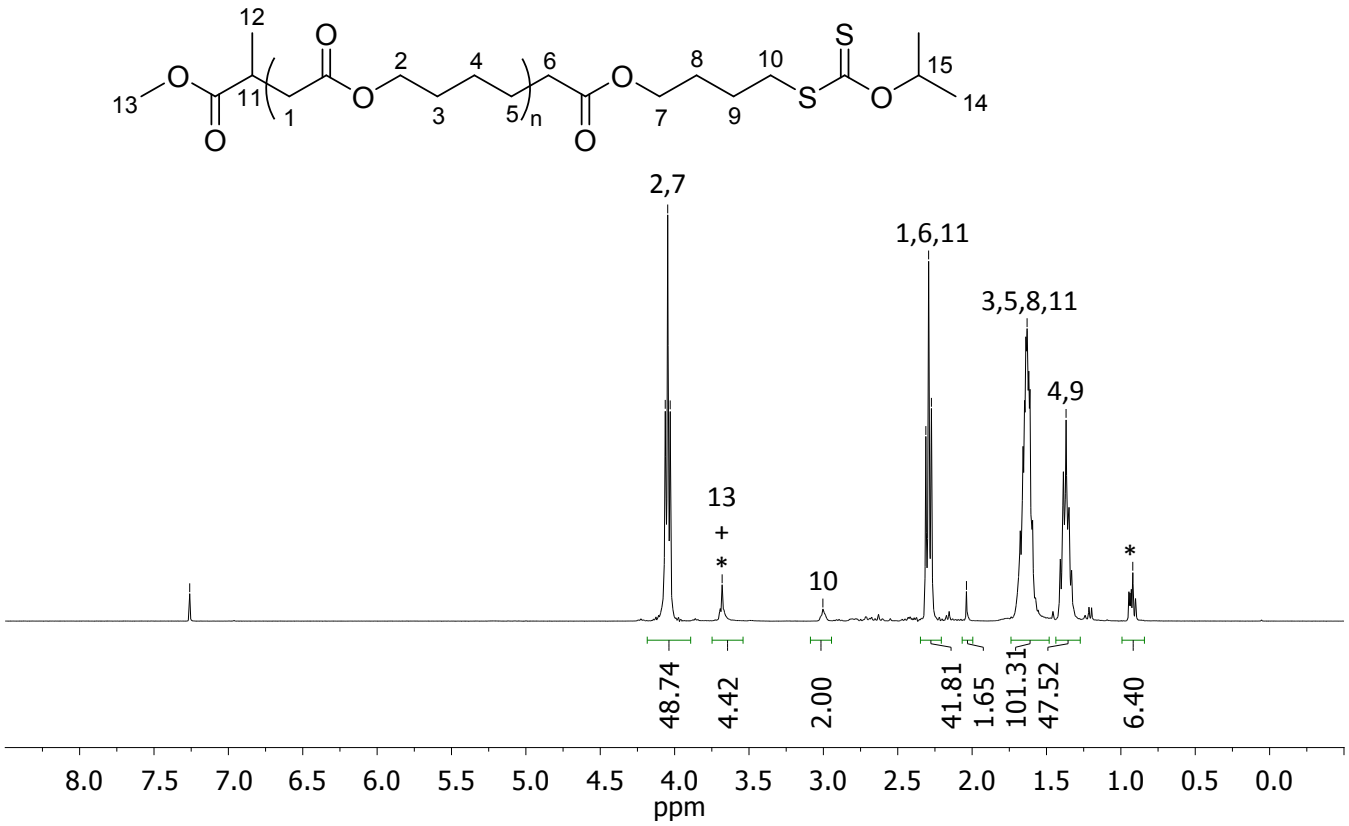

Figure S43 – ^{1}H NMR spectrum of poly(MDO)$_{34}$ formed using CTA **4** (500 MHz, $CDCl_3$). * 1,4- and 1,7-H abstraction side reactions.

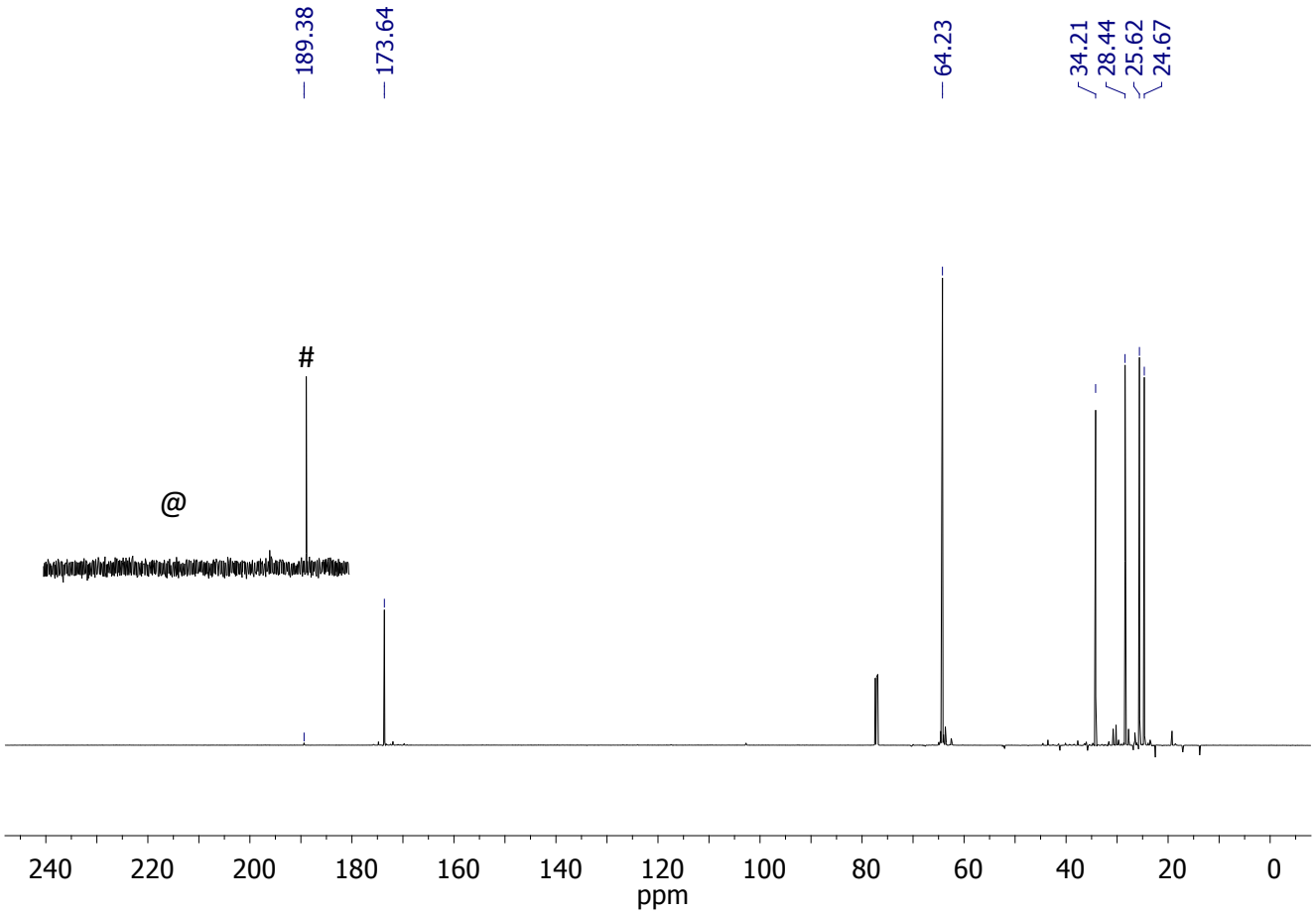

Figure S44 – ^{13}C APT NMR spectrum of poly(MDO)$_{34}$ formed using CTA **4** (125 MHz, $CDCl_3$). Insert: expanded section from δ = 180 – 240 ppm showing: @ - Peak associated with the xanthate; # - Peak associated with the carbonodithioate carbonyl.

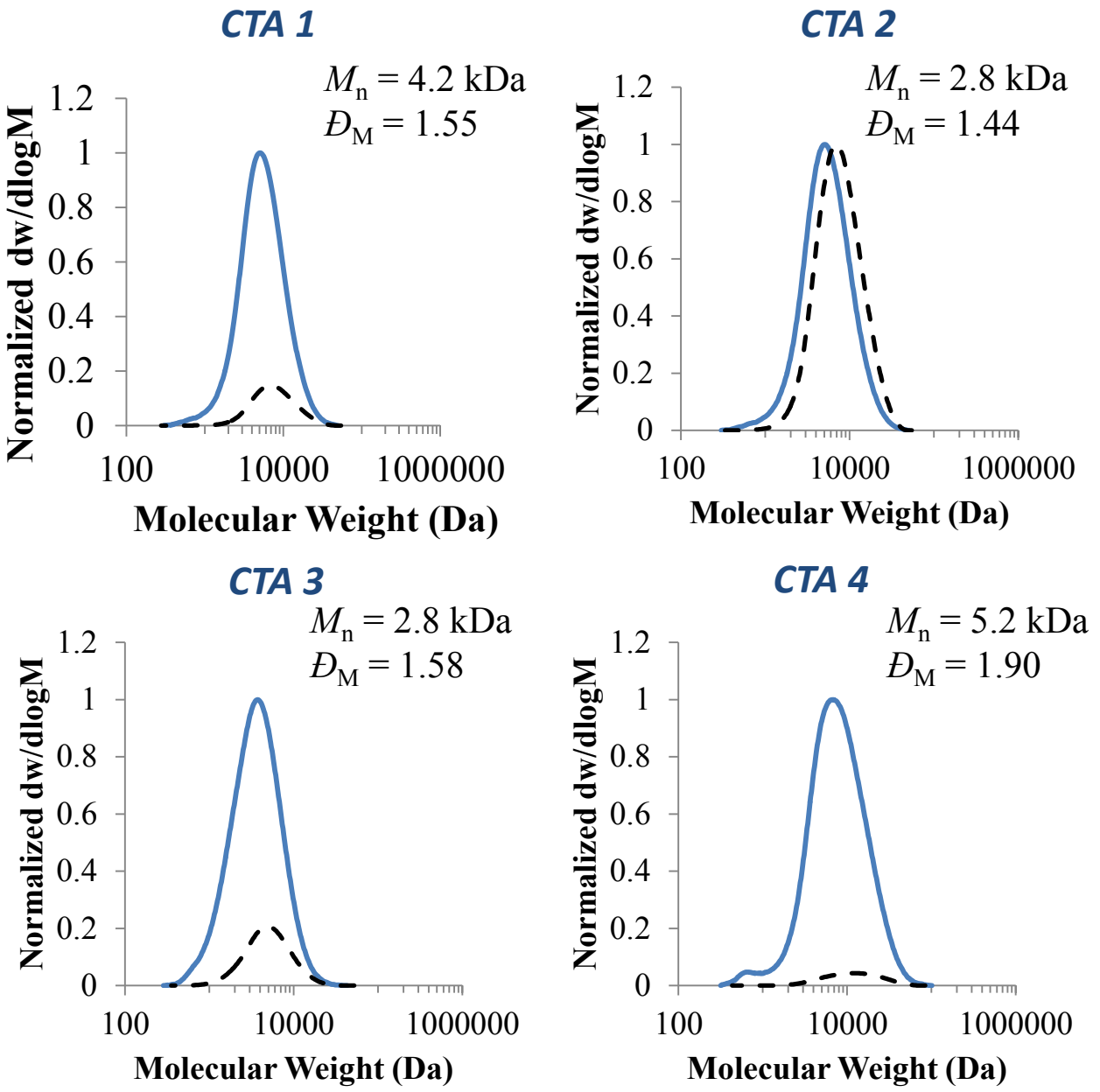

Figure S45 – SEC chromatograms of poly(MDO) formed using all four CTAs. Dashed line (---): UV trace @ 280 nm (normalized to RI signal).

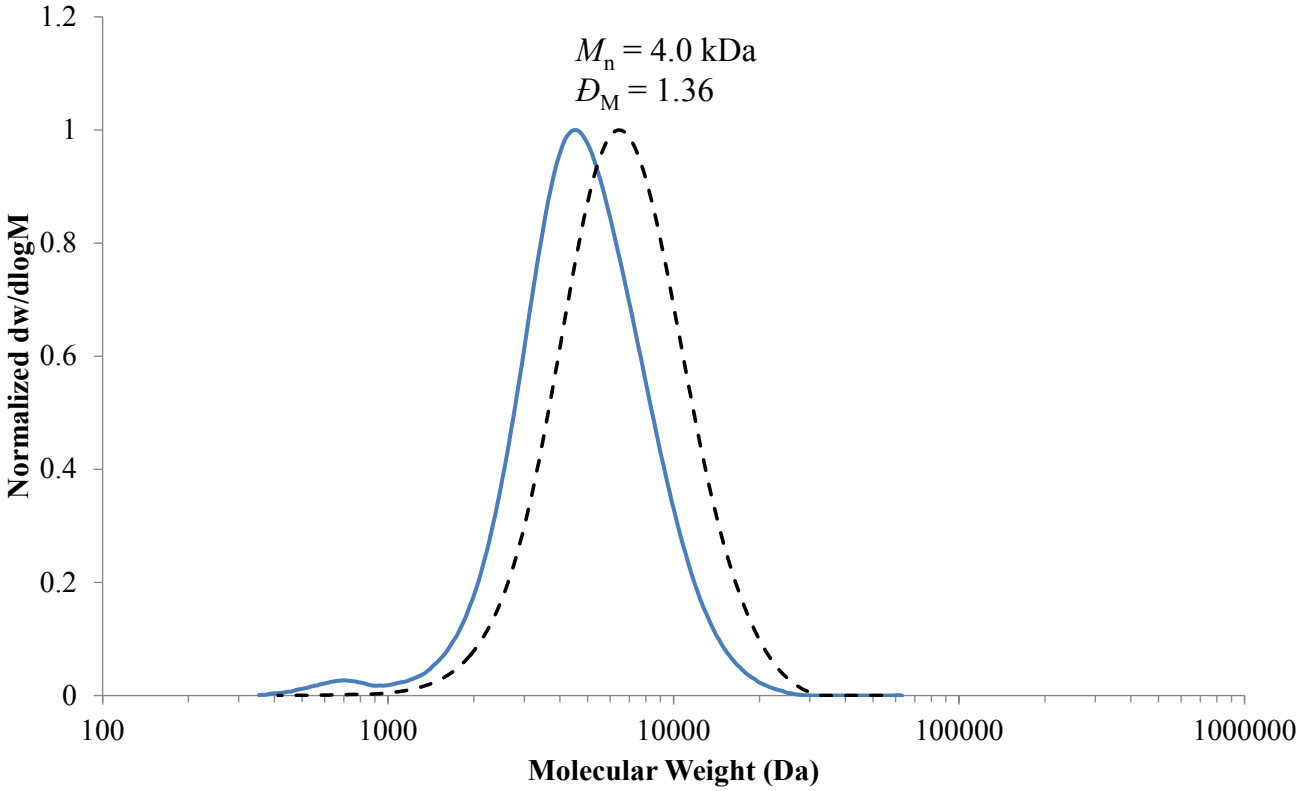

Figure S46 – SEC chromatogram of poly(MDO)$_{14}$ after aminolysis and Michael addition of propargyl methacrylate. M_n = 4.0 kDa, $Đ_M$ = 1.36 (SEC $CHCl_3$, based on PS standards). Dashed line (---): UV trace @ 280 nm (normalized to RI signal).

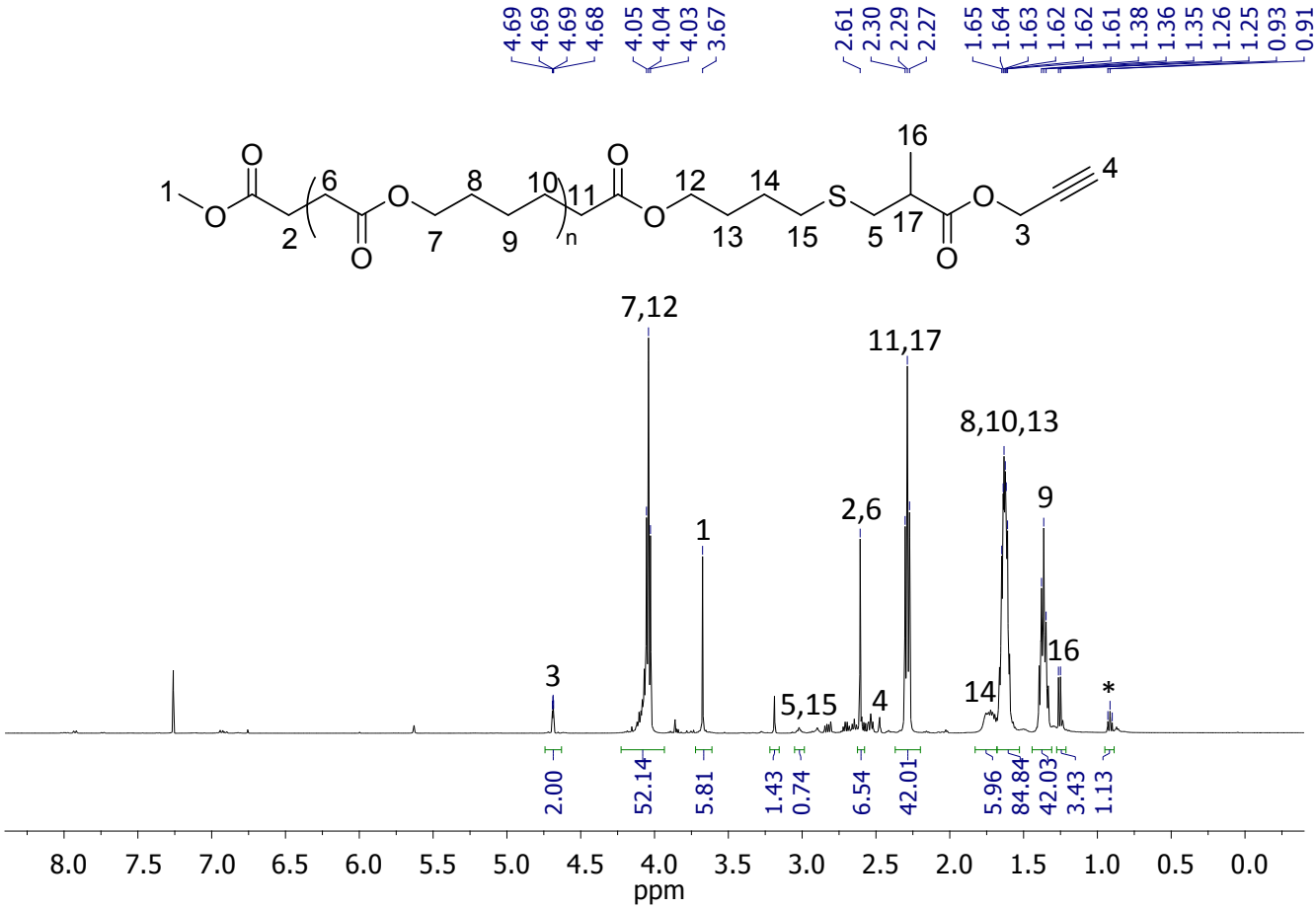

Figure S47 – ^{1}H NMR spectrum of poly(MDO)$_{14}$ after aminolysis and Michael addition of propargyl methacrylate (500 MHz, $CDCl_3$).

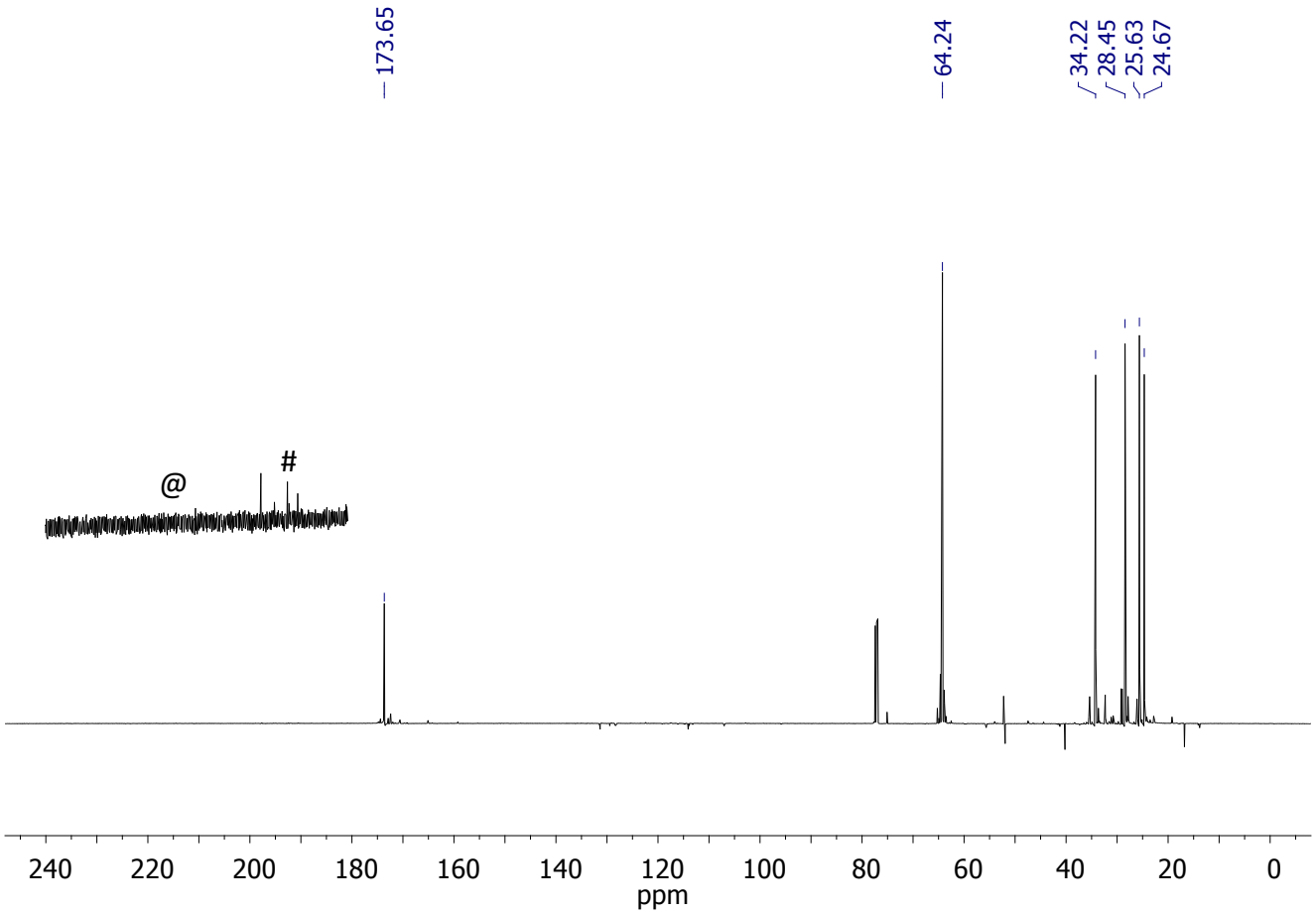

Figure S48 – ^{13}C APT NMR spectrum of poly(MDO)$_{14}$ after aminolysis and Michael addition of propargyl methacrylate (125 MHz, $CDCl_3$). Insert: expanded section from δ = 180 – 240 ppm showing: @ - Peak associated with the xanthate; # - Peak associated with the carbonodithioate carbonyl.

Figure S49 – MALDI-ToF mass spectrum of poly(MDO)$_{14}$ after aminolysis and Michael addition of propargyl methacrylate.

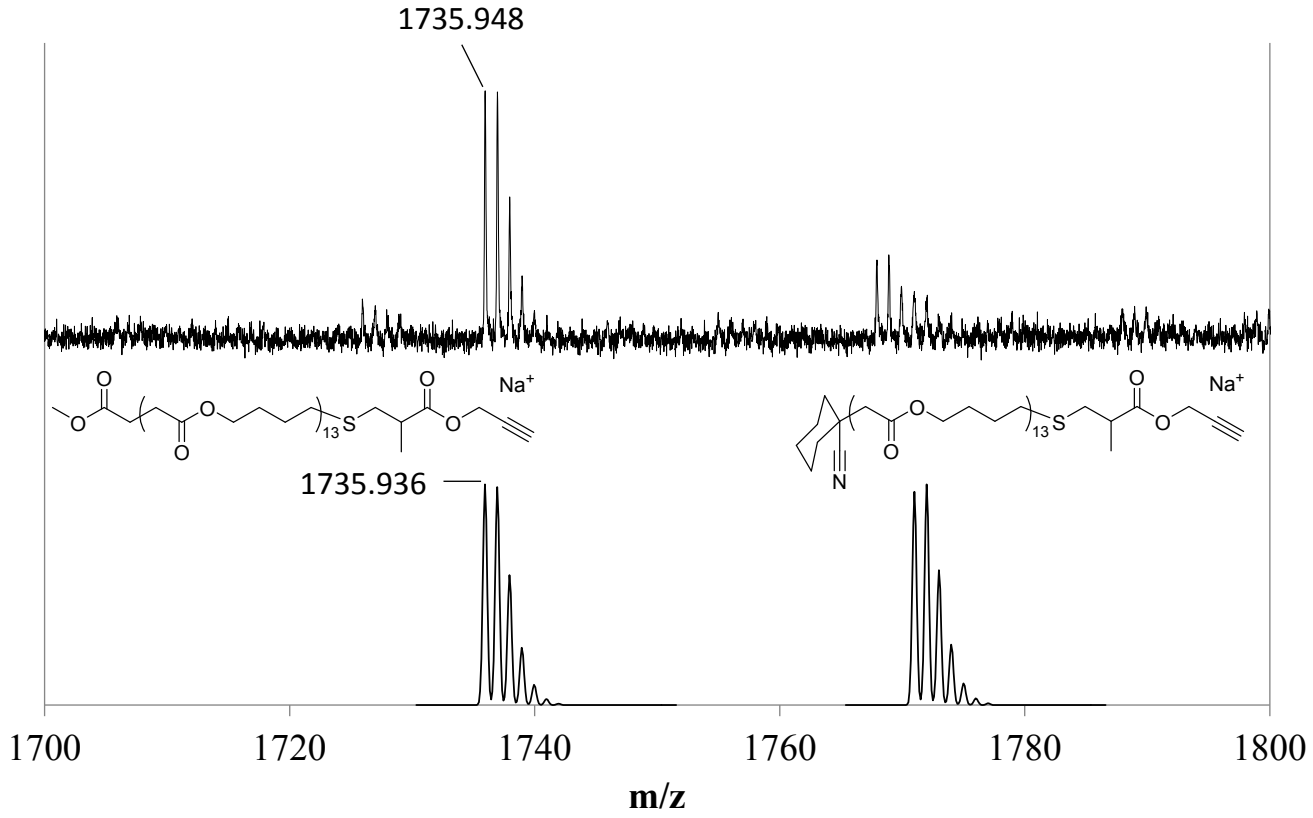

Figure S50 - MALDI-ToF MS isotopic distribution of poly(MDO)$_{14}$ after aminolysis and Michael addition of propargyl methacrylate. Top = measured, bottom = simulated.

References

1. A. R. Katritzky, S. Sobiak and C. M. Marson, *Magn. Reson. Chem.*, 1988, **26**, 665-670.
2. C. Copeland and R. V. Stick, *Aust. J. Chem.*, 1984, **37**, 1483-1487.